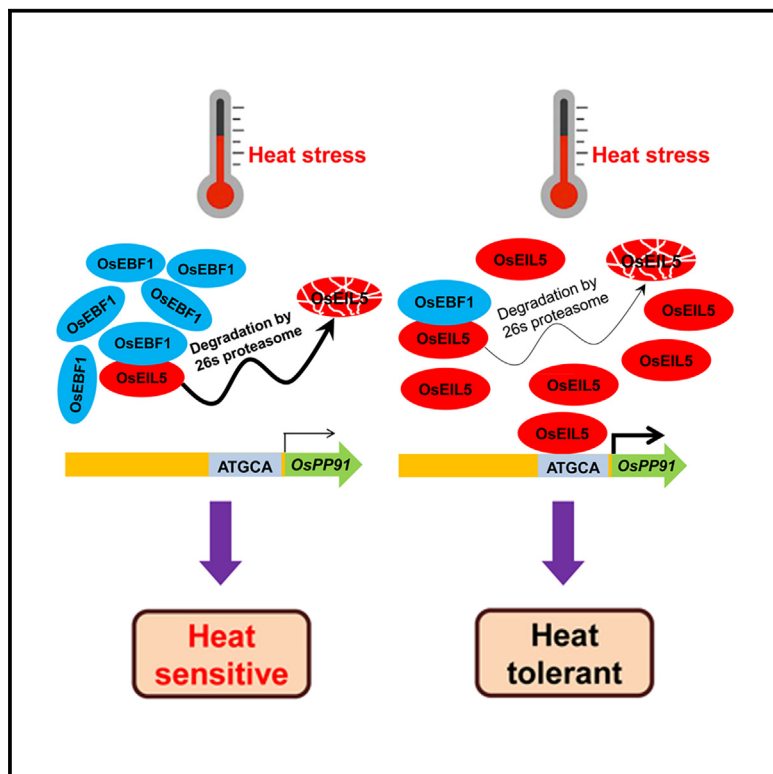


The OsEBF1-OsEIL5-OsPP91 module regulates rice heat tolerance via ubiquitination and transcriptional activation

Graphical abstract



Authors

Jianping Liu, Ke Wang, Guining Wang, ..., Hao Chen, Ya Wang, Weifeng Xu

Correspondence

wfxu@fafu.edu.cn

In brief

Liu et al. demonstrate that the transcription factor OsEIL5 enhances rice tolerance to heat stress at the seedling and reproductive stages by directly activating expression of the target gene OsPP91. An F box protein, OsEBF1, interacts with and degrades OsEIL5, negatively regulating the heat tolerance of rice.

Highlights

- The F box protein OsEBF1 negatively regulates rice thermotolerance
- OsEBF1 interacts with and degrades the transcription factor OsEIL5
- OsEIL5 confers rice tolerance to heat stress at the seedling and reproductive stages
- As the target of OsEIL5, OsPP91 is indispensable for rice heat tolerance



Article

The OsEBF1-OsEIL5-OsPP91 module regulates rice heat tolerance via ubiquitination and transcriptional activation

Jianping Liu,¹ Ke Wang,² Guining Wang,¹ Zhi Peng,³ Tao Wang,³ Yang Meng,³ Jinli Huang,³ Jiaohan Huo,³ Xin Li,¹ Xiaoqi Zhu,¹ Feiyun Xu,¹ Qian Zhang,³ Zhengrui Wang,³ Hao Chen,⁴ Ya Wang,⁵ and Weifeng Xu^{1,6,*}

¹Center for Plant Water-use and Nutrition Regulation and College of JunCao Science and Ecology, Joint International Research Laboratory of Water and Nutrient in Crop, Fujian Agriculture and Forestry University, Fuzhou 350002, China

²Institute of Resources, Environment and Soil Fertilizer, Fujian Academy of Agricultural Sciences, Fuzhou 350000, China

³College of Resources and Environment, Fujian Agriculture and Forestry University, Fuzhou 350002, China

⁴Rice Research Institute, Guangdong Academy of Agricultural Sciences, Guangzhou 510640, China

⁵Cereal Crops Research Institute, Henan Academy of Agricultural Sciences, Zhengzhou 450002, China

⁶Lead contact

*Correspondence: wfxu@fafu.edu.cn

<https://doi.org/10.1016/j.celrep.2025.115271>

SUMMARY

Understanding the regulatory mechanisms underlying the plant heat stress response is important for developing climate-resilient crops, including rice (*Oryza sativa*). Here, we report that OsEIL5, one member of the ETHYLENE INSENSITIVE3-LIKE family, positively regulates rice heat tolerance at the seedling and reproductive stages. OsEIL5 directly binds to the promoter of *OsPP91* (encoding one type 2C protein phosphatase) and activates its expression. *OsPP91* is required for rice thermotolerance, and overexpressing *OsPP91* in *oseil5-1* partially rescues its heat sensitivity. The F box protein OsEBF1 interacts with OsEIL5 and degrades it through the ubiquitination pathway, resulting in the reduction of *OsPP91* expression and ultimately weakening rice heat tolerance. Knocking out *OsEIL5* in the EBF1R13 line partially reduces its extremely high heat tolerance. Taken together, our work uncovers a mechanism that finely regulates rice thermotolerance through the OsEBF1-OsEIL5-OsPP91 module at the posttranslational and transcriptional levels.

INTRODUCTION

Global warming has increased the average temperature of the Earth's surface, making global heat events more intense and having a significant negative impact on crop productivity.^{1,2} It is estimated that for every 1°C increase in global temperature, the global yield of major crops will decrease by 3%–8%.³ Rice is a staple food for more than half of the world's population, and it is susceptible to high-temperature stress during both the seedling and reproductive stages, leading to a decrease in yield and quality. An important way to address this challenge is to explore and utilize genes that control heat tolerance and to cultivate heat-resistant rice varieties.^{4–6}

The only gaseous hormone, ethylene, plays an important role in plants responding to biotic and abiotic stresses.⁷ EIN3 (ETHYLENE INSENSITIVE 3) and EIL (EIN3-like) are core transcription factors of the ethylene signaling pathway.^{7,8} There are six EIL homologs (OsEIL1–OsEIL6) in rice, among which OsEIL1 and OsEIL2 have been clearly confirmed to be involved in ethylene signaling.^{8–11} Research regarding the responses of EIL to biotic stress has mainly concentrated on rice. OsEIL1–OsEIL3 have been reported most frequently, and they influence the disease resistance^{12–14} or BPH (brown planthopper) resis-

tance¹⁵ of rice by directly regulating the expression of downstream target genes. In cassava, MeEIL5 fine-tunes the coordination of melatonin biosynthesis and anti-bacterial activity, which are involved in ethylene-induced disease resistance.¹⁶ It has also been reported that OsEIL1 and OsEIL2 can regulate the resistance of plants to various abiotic stresses; for instance, salt tolerance,^{10,17,18} cold tolerance,¹⁹ and NH₄⁺ efflux.²⁰ The loss-of-function mutants *ethylene receptor 1*, *ein2-ein5*, and *ein3 ein1* each exhibit a lower survival rate compared with wild-type *Arabidopsis* under heat stress,^{21–23} supporting the theory that ethylene signaling is involved in basal thermotolerance. However, it is still unclear whether members of the rice EIL family are involved in responding to heat stress.

Plant protein phosphatases are mainly divided into three categories, among which the main category is type 2C protein phosphatase (PP2C), which requires Mn²⁺ or Mg²⁺ to exert activity.²⁴ In rice, among the 90 predicted PP2Cs, only a few have been reported to be involved in the resistance of rice to drought,^{25–27} disease,^{28,29} osmotic and salt stress,³⁰ and aluminum stress.³¹ A recent report shows that the cassava phosphatase MePP2C1 modulates thermotolerance by fine-tuning dephosphorylation of antioxidant enzymes.³² Despite these intriguing results, the specific roles of most of the PP2C are still



largely unknown, and no rice PP2C involved in heat stress has been reported.

In the current study, we find that *OsEIL5* has the highest degree of heat stress induction. *OsEIL5* encodes one transcription factor and positively regulates rice heat tolerance at the seedling and reproductive stages, but it probably does not participate in ethylene signal transduction. *OsEIL5* can directly bind to the promoter of the target gene *OsPP91* and activates its expression. Knockout of *OsPP91* reduces rice thermotolerance, and overexpressing *OsPP91* in the *oseil5* mutant partially rescues its heat sensitivity. The F box protein *OsEBF1* interacts with *OsEIL5* and degrades it through the ubiquitination pathway, resulting in the reduction of *OsPP91* expression, ultimately weakening rice heat tolerance. Deletion of *OsEIL5* in the *EBF1R13* strain only partially reduces its extremely high heat tolerance. Our findings greatly expand our understanding of heat stress responses in rice and might provide genetic resources for breeding heat-tolerant rice varieties.

RESULTS

Loss of function of *OsEIL5* confers heat sensitivity in rice

Among the six *EIL* genes, *OsEIL1*, *OsEIL2*, and *OsEIL5* were obviously induced by heat stress, and their expression levels reached the highest values at 3 or 6 h after heat treatment and then began to decrease. The other three genes (*OsEIL3/4/6*) had weaker responses to heat stress (Figure 1A). The highest degree of heat induction was observed in *OsEIL5* (about 22-fold), followed by *OsEIL2* and *OsEIL1* (Figure 1A), suggesting that *OsEIL5* is likely to play an important role in the response of rice to heat stress, so our follow-up study focused on this gene. Next, we investigated the responses of *OsEIL5* to various environmental stimuli. Beside the constitutive expression in the assayed samples, the expression of *OsEIL5* was significantly upregulated by polyethylene glycol (PEG), abscisic acid (ABA), and heat stress, while 1-aminocyclopropanecarboxylic acid (ACC) and cold stress had no effects (Figure 1B).

To investigate the potential biological function of *OsEIL5* in rice heat response, two independent mutants were generated using CRISPR-Cas9.³³ The *oseil5-1* mutant had a 1-bp insertion, and the *oseil5-2* mutant had a 1-bp deletion, both of which led to a premature stop (Figures S1A and S1B). When treated with heat stress (45°C for 24 h), compared with ZH11, both *oseil5-1* and *oseil5-2* were more sensitive to heat stress. The survival rates for *oseil5-1*, *oseil5-2*, and ZH11 were 10.4%, 39.6%, and 91.4%, respectively (Figures 1C and 1D). At the same time, *oseil5* accumulated more H₂O₂ than ZH11 under heat stress (Figure 1E). The electrolytic leakage of *oseil5* was also higher than that of ZH11 (Figure 1F). We conclude that *OsEIL5* is of great significance for the heat tolerance of rice seedlings.

***OsEIL5* increases rice heat tolerance at both seedling and reproductive stages**

Next, we overexpressed *OsEIL5* in ZH11 and generated several transgenic lines. Two independent overexpression (OE) lines (OE7-1 and OE9-3) were selected for heat tolerance testing (45°C for 48 h) (Figure 2A). Under heat stress, both OE7-1 and OE9-3 were more tolerant than ZH11, which was just opposite

to the heat-sensitive phenotype of *oseil5*. The survival rates after recovery for OE7-1, OE9-3, and ZH11 were 63.0%, 63.3%, and 21.7%, respectively (Figures 2B and 2C). Consistently, OE7-1 and OE9-3 accumulated less H₂O₂ than ZH11 under heat stress (Figure 2D). The electrolytic leakage of OE7-1 and OE9-3 was also lower than that of ZH11 (Figure 2E).

Rice is highly sensitive to high-temperature stress, especially at the reproductive stage,³⁴ and improving thermotolerance at this stage is of particular importance to reduce yield loss. Therefore, we performed high-temperature treatment at this stage. The seed-setting rates of *oseil5* were less than 20% (16.5% for *oseil5-1* and 17.2% for *oseil5-2*), the seed-setting rate of ZH11 was only 41.2%, while that of two *OsEIL5*-OE lines could exceed 70% (71.5% for OE7-1 and 75.3% for OE9-3) after treatment at 40°C for 7 days (Figures 2F and 2G). Under normal conditions, there were no significant differences in seed-setting rates among these materials (Figures 2F and 2G). These results demonstrate that *OsEIL5* plays an important and positive role in rice thermotolerance at the seedling and reproductive stages.

To test whether the enhanced thermotolerance of *OsEIL5*-OE affects rice growth, we assessed key agronomic traits in ZH11, OE7-1, and OE9-3 under field conditions. The yield-related traits (plant height, tiller number, heading date, 1,000-grain weight, and grain yield per plant) were similar across the genotypes (Figures S2A–S2E). In addition, grain width and grain length were almost the same between *OsEIL5*-OE and ZH11 (Figures S2F–S2H). These results indicate that the gain of *OsEIL5* function does not incur a growth penalty in rice.

***OsEIL5* is located in the nucleus and is capable of transcriptional activation**

To study the subcellular localization of *OsEIL5*, we delivered the construct expressing *OsEIL5*-EGFP into the epidermis of tobacco. The transgenic recipient is a nuclear marker line expressing RFP (red fluorescent protein) fused with histone 2B.³⁵ According to the EGFP signal, *OsEIL5* was mainly localized to the nucleus (Figure 3A). The transient expression of *OsEIL5*-EGFP in rice protoplasts has substantiated the nuclear localization of *OsEIL5* (Figure 3B).

OsEIL1–OsEIL3 have been reported as transcription factors that can activate the expression of the corresponding target genes.^{10,14} *OsEIL5* also contains a conserved EIN3 domain like *OsEIL1–OsEIL3*. Based on this, we divided *OsEIL5* into three segments: N terminus, middle part, and C terminus (Figure 3C). To verify whether *OsEIL5* has the same activation ability as *OsEIL1–OsEIL3*, the full-length *OsEIL5* was fused to the GAL4 DNA-binding domain (BK-*OsEIL5*). Like the positive control, the yeast cells co-transformed with empty GAL4 DNA-activating domain (AD), and BK-*OsEIL5* vectors could grow normally on quadruple dropout medium, while the negative control could not (Figure 3D). Next, five different truncated forms of *OsEIL5* were fused to the GAL4 DNA-binding domain. Compared with the negative control, only the fusion proteins containing the C terminus (C or middle plus C terminus, C or MC) had transcriptional activation activity in yeast cells (Figures 3C–3E). These results suggest that *OsEIL5* is a nuclear transcriptional activator and that its transcriptional activity depends on the amino acids in the C-terminal region from 339 to 504.

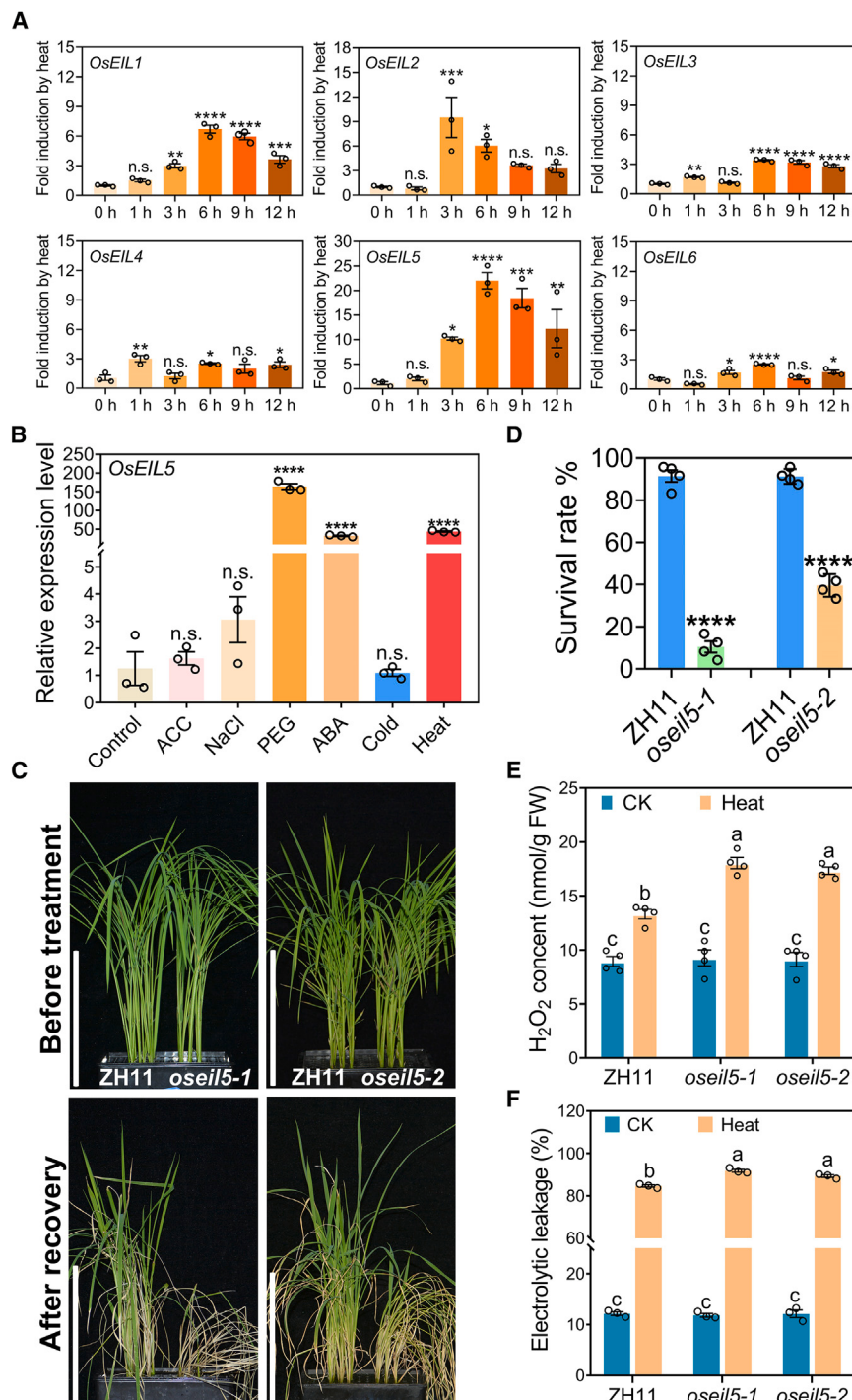


Figure 1. The osei5 mutants are hypersensitive to high temperature

(A) OsEIL expression at different times after heat stress.

(B) Upregulation of OsEIL5 by hormones and abiotic stresses.

(C) The heat-sensitive phenotype of osei5. Scale bars: 12.5 cm

(D) Statistical analysis of survival rate in (C) after heat treatment and recovery.

(E and F) H₂O₂ content (E) and electrolytic leakage (F) in ZH11 and osei5 before and after heat treatment.

In (A), (B), and (D), data represent means \pm SE; $n = 3$ or 4 ($^*p < 0.05$, $^{**}p < 0.01$, $^{***}p < 0.001$, $^{****}p < 0.0001$; n.s., not significant at $p < 0.05$; Student's t test). In (E) and (F), data represent means \pm SE; $n = 4$ or 3. Different letters above the bars indicate differences by one-way ANOVA with Tukey's multiple-comparisons test at $p < 0.05$. See also Figures S1A and S1B.

showed root and shoot lengths similar to ZH11 (Figures S2I and S2J). Similar phenomena were observed when treated with the ethylene analog ethephon (Figures S2K and S2L). These data suggest that OsEIL5 may have no significant effects on the ethylene response of rice.

To identify the candidate genes regulated by OsEIL5, we searched the RiceTFTtarget database (<https://cbi.njau.edu.cn/RiceTFTtarget/>).³⁶ Among the 189 predicted candidate genes (Table S1), there are seven genes with a prediction score of ≥ 0.5 in machine learning. Two genes encode retrotransposons; three genes encode expressed proteins without functional annotation; one gene (Os01g0805400), Os6, encodes cytokinin-N-glycosyltransferase³⁷; and one gene (Os06g0698300), OsPP91, encodes PP2C.²⁷ Li et al.³⁸ report that UGT76C2, a protein homologous to Os6 in *Arabidopsis*, improves drought and salt tolerance of rice. OsPP18, which is closely related to OsPP91, has been reported to positively modulate drought and oxidative stress tolerance in rice.²⁷ So we focused on these two genes. Compared to ZH11, OsPP91 was significantly upregulated, whereas Os6 was almost unchanged in

OsEIL5 directly activates OsPP91 transcription

Before explaining how OsEIL5 affects heat tolerance, we need to clarify whether OsEIL5 is involved in ethylene response. ZH11, osei5, and OsEIL5-OE were treated with ACC. After treatment, they all showed significantly shortened roots,¹⁰ but there was no obvious elongation in shoots. More importantly, regardless of whether ACC was present, osei5 and OsEIL5-OE

OsEIL5-OE (Figures 4A and 4B). The log₂ TPM (transcripts per million) results downloaded from the database show that OsEIL5 and OsPP91 are co-expressed in multiple rice tissues (Figure S3A). Furthermore, OsPP91 was obviously up-regulated by heat in ZH11 (about 10-fold). However, the fold induction of OsPP91 was not significant in osei5-1 (Figure 4C), implying that OsPP91 is likely to be the target of OsEIL5.

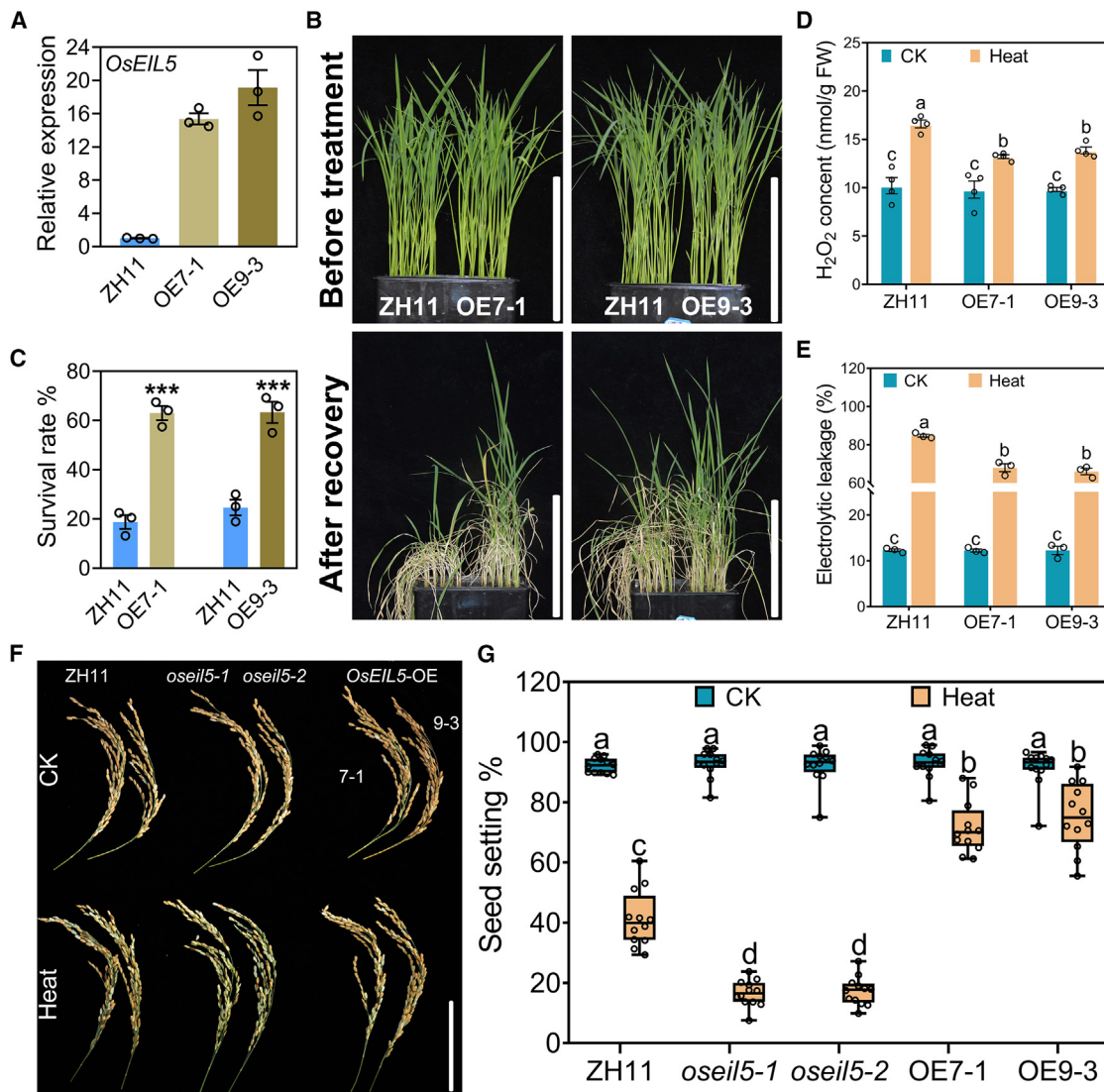


Figure 2. OsEIL5 positively regulates rice heat tolerance at the seedling and reproductive stages

(A) OsEIL5 expression in two OsEIL5-OE lines.

(B) Heat-tolerant phenotype of OsEIL5-OE lines. Scale bars: 12.5 cm

(C) Statistical analysis of survival rate in (B) after heat treatment and recovery.

(D and E) H₂O₂ content (D) and electrolytic leakage (E) in ZH11 and OsEIL5-OE before and after heat treatment.

(F and G) Comparison of thermotolerance among ZH11, osei5, and OsEIL5-OE at the reproductive stage. Scale bar: 10 cm.

In (A) and (C), data represent means \pm SE; $n = 3$ ($^{***}p < 0.001$, Student's t test). In (D), (E), and (G), data represent means \pm SE; $n = 4, 3$, or 12. Different letters above the bars indicate differences by one-way ANOVA with Tukey's multiple-comparison test at $p < 0.05$. See also Figures 2A–2H.

To determine whether OsEIL5 functions as a direct regulator of OsPP91, we analyzed the sequence of OsPP91 and identified five EIN3-binding motifs (EBM1–EBM5; ATGT/CA) in the promoter (Figure 4D). Hence, we performed a chromatin immunoprecipitation (ChIP) assay using transgenic plants harboring FLAG-tagged OsEIL5 (OsEIL5-3×FLAG). As shown in Figure 4E, an anti-FLAG antibody precipitated the pChIP-A fragment instead of the pChIP-B and pChIP-C fragments. The yeast one-hybrid (Y1H) analysis disclosed that OsEIL5 interacts with the p2 fragment containing EBM1 (Figure 4F). Subsequently, we conducted an electrophoretic mobility shift

assay (EMSA) with glutathione S-transferase (GST)-OsEIL5 protein expressed in *Escherichia coli*. As shown in Figure 4G, GST-OsEIL5 directly bound to DNA probes containing EBM1 (p3), which is present in the pChIP-A, but it did not bind to the DNA probes with mutated EBM1. The specificity of binding was confirmed by a competition assay using an unlabeled competitor probe (Figure 4G).

To examine whether OsEIL5 could indeed activate OsPP91 expression *in planta*, we cloned the 1,550 bp promoter sequences (p1) upstream of ATG into the luciferase (LUC) reporter gene (pOsPP91:LUC). Compared with the co-transfected EGFP

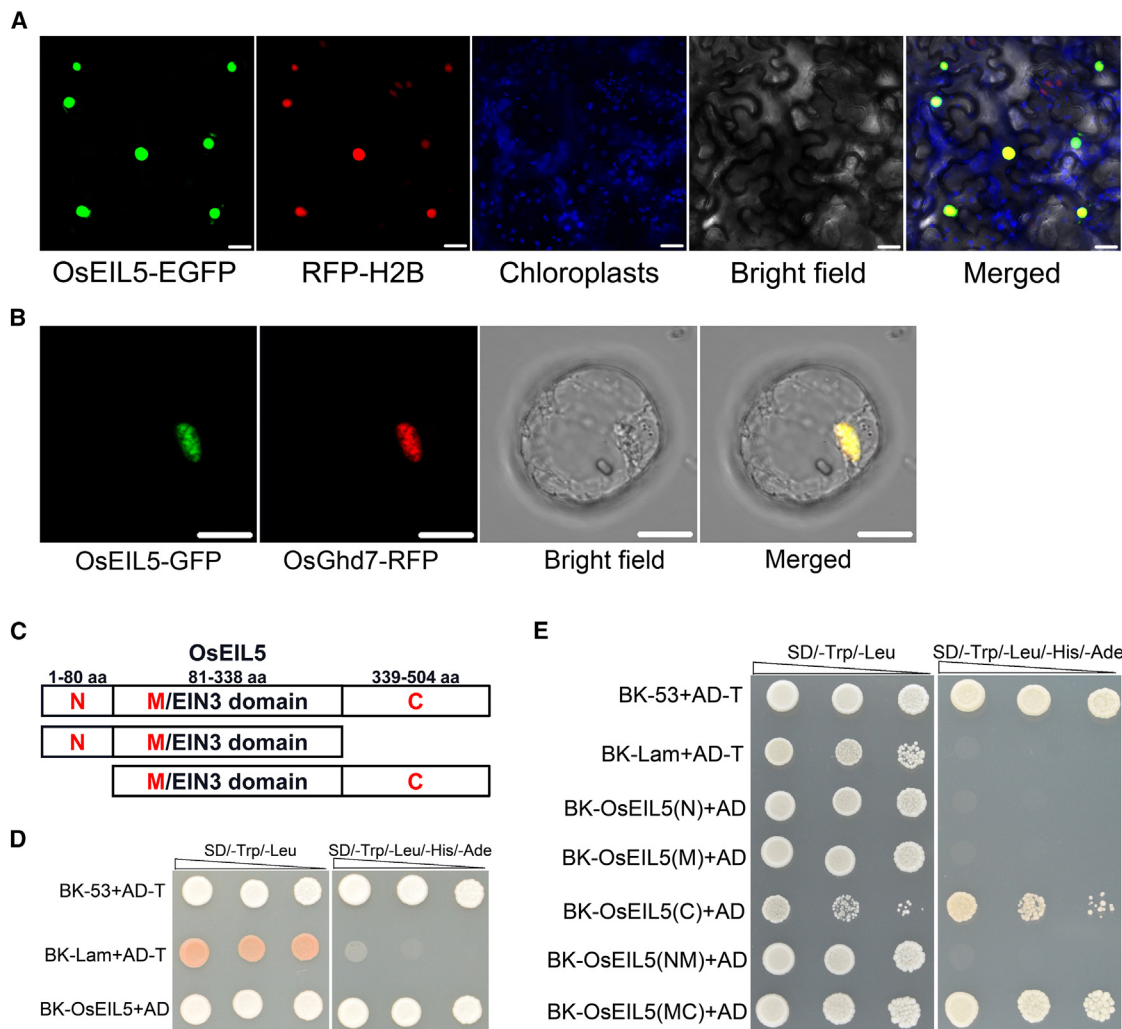


Figure 3. Subcellular localization and transcriptional activation of OsEIL5

(A) Subcellular localization of OsEIL5 in leaves of *N. benthamiana*. Scale bars: 25 μ m
 (B) Subcellular localization of OsEIL5 in rice protoplasts. Scale bars: 10 μ m
 (C) Protein domain structure of OsEIL5. N, N terminus; M, middle; C, C terminus.
 (D and E) Transcriptional activation assay of OsEIL5 in yeast.

and pOsPP91:LUC reporter control, the co-transfected effector of OsEIL5-EGFP significantly increased OsPP91 promoter-driven LUC activities (Figures S3B and S3C). These results indicate that OsEIL5 directly binds to the OsPP91 promoter *in vivo* and *in vitro* and activates its transcription.

OsEIL5 confers rice thermotolerance partially through OsPP91

Since OsEIL5 activated OsPP91 transcription, we hypothesized that OsPP91 may have a similar role as OsEIL5 in heat response. To confirm this, we obtained the ospp91 mutants using CRISPR-Cas9 (Figures S1C and S1D). When treated with 45°C for 24 h, ospp91-1 and ospp91-2 exhibited higher sensitivity than ZH11. The survival rates for ospp91-1, ospp91-2, and ZH11 were 15.3%, 16.7%, and 89.8%, respectively (Figures 5A and 5B). Under heat stress, ospp91 accumulated more H₂O₂ than ZH11 (Fig-

ure 5C). The electrolytic leakage of ospp91 was also higher than that of ZH11 (Figure 5D). We conclude that OsPP91 is also important for heat tolerance of rice seedlings.

To further confirm whether OsPP91 functions downstream of OsEIL5, we overexpressed OsPP91 in osei5-1. Three independent osei5-1/OsPP91-OE lines (#3, #5, and #8) were selected for heat tolerance testing (45°C for 24 h). In the three lines, the transcription levels of OsPP91 were 201.2, 472.6, and 140.4 times higher, respectively, than that in ZH11, while the OsPP91 expression in osei5-1 was only about 30% of that in ZH11 (Figure 5E). Under heat stress, the osei5/OsPP91-OE lines were more tolerant than osei5-1, and more sensitive than ZH11. The survival rates for ZH11, osei5-1, #3, #5, and #8 were 90.3%, 8.3%, 37.5%, 47.2%, and 23.6%, respectively (Figures 5F and 5G). The results show that overexpressing OsPP91 can partially rescue the heat sensitivity of osei5-1 and that the heat tolerance

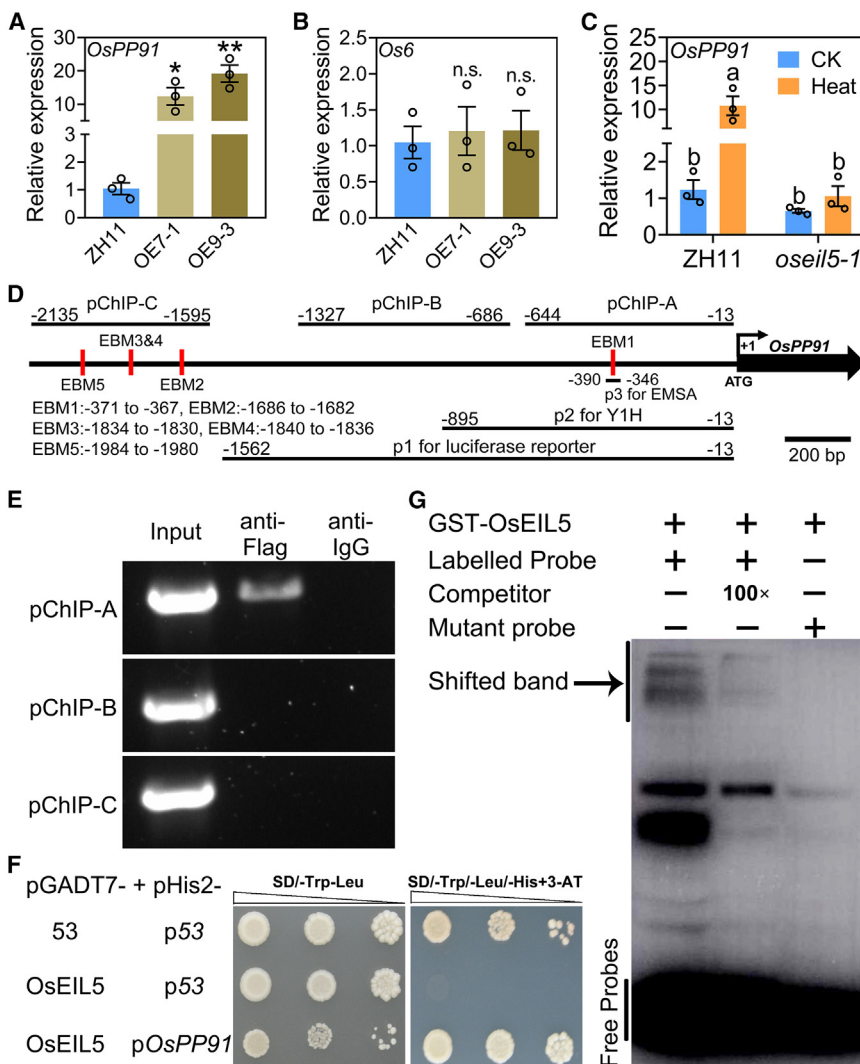


Figure 4. OsEIL5 directly binds to the promoter of OsPP91 to activate its expression

(A and B) *OsPP91* (A) and *Os6* (B) expression in two *OsEIL5*-OE lines under normal growth conditions. Data represent means \pm SE; $n = 3$ (* $p < 0.05$, ** $p < 0.01$; n.s., $p < 0.05$; Student's t test).

(C) Fold induction of *OsPP91* by heat stress in ZH11 and *osei5-1*. Data represent means \pm SE; $n = 3$. Different letters above the bars indicate differences by one-way ANOVA with Tukey's multiple-comparisons test at $p < 0.05$.

(D) Schematic of putative EBM (ATGT/CA) in the *OsPP91* promoter. pChIP-A, -B, and -C are fragments used for ChIP. p1 is the construct of the luciferase (LUC) reporter, p2 is for the Y1H assay, and p3 is for the EMSA. The red boxes indicate putative EBM, and the black lines indicate the promoter sequence.

(E) ChIP assay showing that OsEIL5 can bind the *OsPP91* promoter *in vivo*. DNA from the roots of seedlings expressing 3xFLAG-tagged OsEIL5 lines at the 2.5- to 3.5-leaf stage were immunoprecipitated by anti-FLAG or anti-immunoglobulin G (IgG). The precipitated chromatin fragments were analyzed by PCR using three primer sets (pChIPA-pChIPC) amplifying three *OsPP91* promoter regions, as indicated in (D). One-tenth of the input chromatin was analyzed.

(F) OsEIL5 binds the *OsPP91* promoter in yeast. The pGADT7 plasmid containing the full-length coding sequence of OsEIL5 (pGADT7-OsEIL5) and the pHis2 plasmid containing the p2 fragment of *OsPP91* promoter (pHis2-p*OsPP91*) were co-transformed into yeast cells (Y187). Yeast cells co-transformed with the pGADT7-53/pHis2-p53 or pGADT7-OsEIL5/pHis2-p53 vector were used as the positive or negative control, respectively.

(G) EMSA using normal (ATGCA) and mutated EBM (GGAGC) in p3 with GST-tagged OsEIL5 fusion protein (GST-OsEIL5). Protein was incubated with biotin-labeled DNA fragments (probe) and tested for competition by adding an excess of unlabeled probe (competitor) and for specificity with a labeled mutant probe. Three biological replicates were performed with similar results. See also Figure S3.

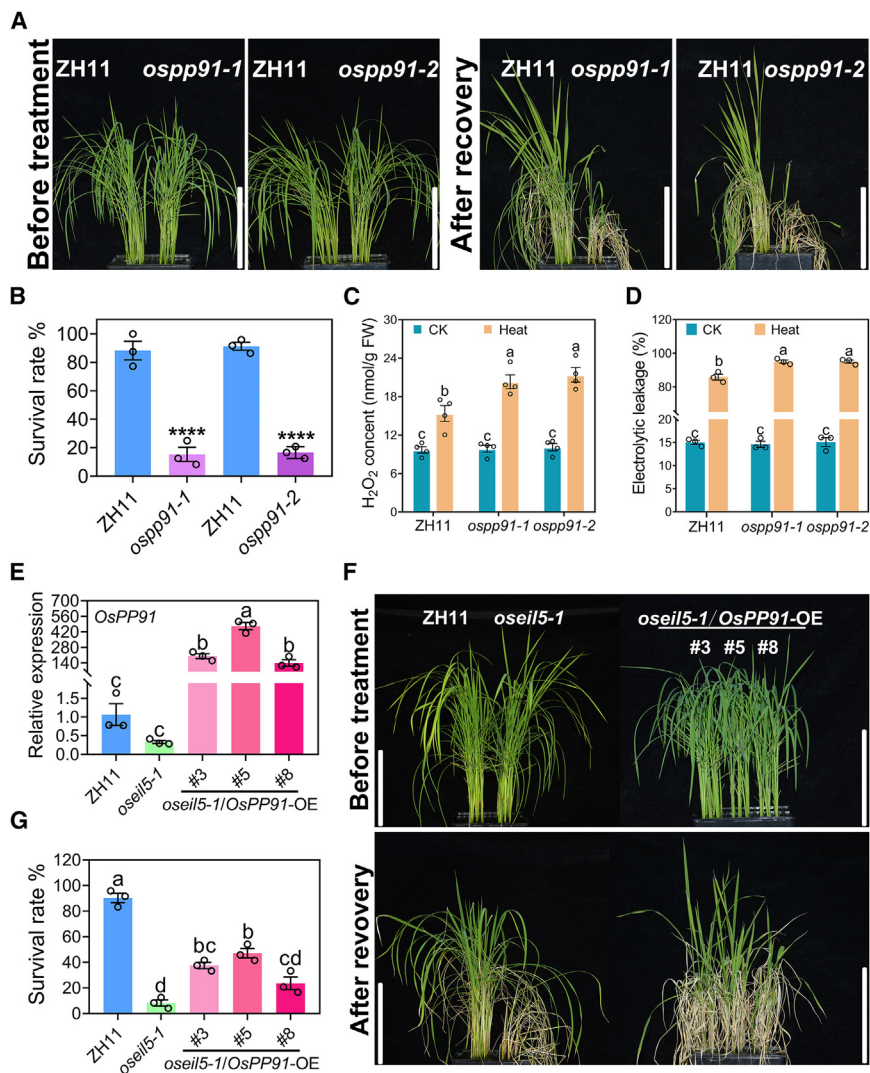
of rice conferred by OsEIL5 was not entirely dependent on *OsPP91*.

OsPP91 belongs to group F2 of the PP2C family rather than group A, which contains ABI1, ABI2, HAB1, and HAB2, known as negative regulators of ABA signaling.^{27,39} To determine whether *OsPP91* is involved in ABA signaling, we treated ZH11 and *ospp91* with ABA. After treatment, they all showed significantly shortened roots and shoots. Importantly, regardless of whether ABA was present, *ospp91* showed root and shoot lengths similar to ZH11 (Figures S4A–S4C). Furthermore, we also found that the ABA sensitivity of *osei5* and *OsEIL5*-OE was not different compared with ZH11 (Figures S4D–S4F), even though the expression of *OsPP91* in these materials was downregulated or significantly upregulated, respectively (Figures 4A and 5E). These results together suggest that the function of OsEIL5 and *OsPP91* in response to heat stress may be ABA independent.

OsEIL5 regulates heat stress-responsive genes in rice

To find more genes regulated by OsEIL5 during heat response, we compared gene expression profiles using RNA sequencing (RNA-seq). In ZH11, after heat stress, 2,485 and 3,376 genes were significantly upregulated ($\log_2\text{FC}$ [fold change] ≥ 1 , $q \leq 0.05$) and downregulated ($\log_2\text{FC} \leq 1$, $q \leq 0.05$), respectively. Among them, 607 and 860 genes were not significantly upregulated or downregulated in *osei5-1* (Figure S5A; Table S2). Because OsEIL5 is a transcriptional activator (Figures 3, 4, and S3), we considered these 607 upregulated genes OsEIL5-dependent heat stress-responsive genes. However, *OsPP91* was not identified among the 607 genes.

KEGG (Kyoto Encyclopedia of Genes and Genomes) enrichment analysis showed that the abovementioned 607 genes are enriched in protein processing in the endoplasmic reticulum (ER), indole alkaloid biosynthesis, and oxidative phosphorylation (Figure S5B). Heat stress causes the accumulation of misfolded proteins in the



ER, triggering the unfolded protein and ER stress response,⁴⁰ so we selected 9 genes related to protein processing in the ER and performed RT-qPCR. These genes, encoding the ER protein chaperone BiP1 (Os02g0115900), Hsp71.1 (Os03g0276500), thiol-disulfide oxidoreductase (Os03g0733800), calreticulin precursors (Os03g0832200 and Os04g0402100), OsUbc46 (Os06g0193000), zinc-finger protein (Os06g0639100), dimerization domain-containing protein (Os09g0273800), and Skp1 dimerization domain-like protein (Os12g0595600), were significantly upregulated more than 2-fold by heat stress in ZH11 (Figure S5C). However, the fold induction rates of these genes in *osei5-1* after heat stress were obviously lower than those in ZH11 (Figure S5C). Further detection showed that most of them had higher expression in *OsEIL5-OE* even under normal conditions (Figure S5D). Therefore, we find that besides *OsPP91*, *OsEIL5* also modulates the expression of some other heat-responsive genes, especially those involved in protein processing in the ER.

Then, we tested the resistance of *OsEIL5*-transgenic lines to ER stress. When treated with dithiothreitol (DTT; an inducer

Figure 5. Overexpressing *OsPP91* partially rescues the heat sensitivity of the *osei5-1* mutant

(A) Heat-sensitive phenotypes of the *ospp91* mutants. Scale bars: 12.5 cm

(B) Statistical analysis of survival rate in (A) after heat treatment and recovery. Data represent means \pm SE; $n = 3$ ($***p < 0.0001$, Student's t test).

(C) and (D) H₂O₂ content (C) and electrolytic leakage (D) in ZH11 and *ospp91* before and after heat treatment.

(E) *OsPP91* expression in *osei5-1* and three *osei5-1/OsPP91-OE* (#3, #5, and #8) lines.

(F) Heat stress phenotypes of the *osei5-1/OsPP91-OE* lines. Scale bars: 12.5 cm

(G) Statistical analysis of survival rate in (F) after heat treatment and recovery.

In (C)–(E) and (G), data represent means \pm SE; $n = 4$ or 3. Different letters above the bars indicate differences by one-way ANOVA with Tukey's multiple-comparisons test at $p < 0.05$. See also Figures S1C and S1D.

of ER stress), OE7-1 exhibited stronger resistance than ZH11, whereas *osei5-1* was more susceptible. The survival rates after recovery were 42.3% (ZH11), 74.7% (OE7-1), and 12.7% (*osei5-1*), respectively (Figures S5E and S5F). This finding suggests that *OsEIL5* positively regulates the ER stress resistance of rice, which may contribute to its role in responding to heat stress.

OsEBF1 interacts with OsEIL5 and negatively regulates heat tolerance in rice

To further clarify the molecular mechanisms of *OsEIL5* in regulating thermotolerance, we predicted the possible *OsEIL5*

interaction properties in the STRING (search tool for recurring instances of neighbouring genes) database (<https://cn.string-db.org/>). The result showed that *OsEIL5* may interact with a variety of proteins (Figure S6A). Among them, *OsEBF2* (Os02g0200900) is a homologous protein of *OsEBF1* (Os06g0605900), and both belong to EIN3-binding F box proteins and negatively regulate rice BPH resistance by interacting with *OsEIL1*.^{15,41} To further confirm the interaction, we performed yeast two-hybrid Y2H analysis. As shown in Figure 6A, *OsEIL5* is only physically associated with *OsEBF1* rather than *OsEBF2* in yeast. Next, firefly split-luciferase complementation imaging (LCI) assay was carried out to consolidate the interaction between the two. A strong fluorescence signal was observed in tobacco leaf regions co-expressing *OsEIL5-nLUC/cLUC-OsEBF1* or *OsEBF1-nLUC/cLUC-OsEIL5* but not in the regions co-expressing *OsEIL5-nLUC/cLUC-OsEBF2* or *OsEBF2-nLUC/cLUC-OsEIL5* (nLUC, N-terminal of luciferase; cLUC, C-terminal of luciferase) (Figure 6B). BiFC (bimolecular fluorescence complementation) experiments were performed to determine where *OsEIL5* and *OsEBF1* interact in plant

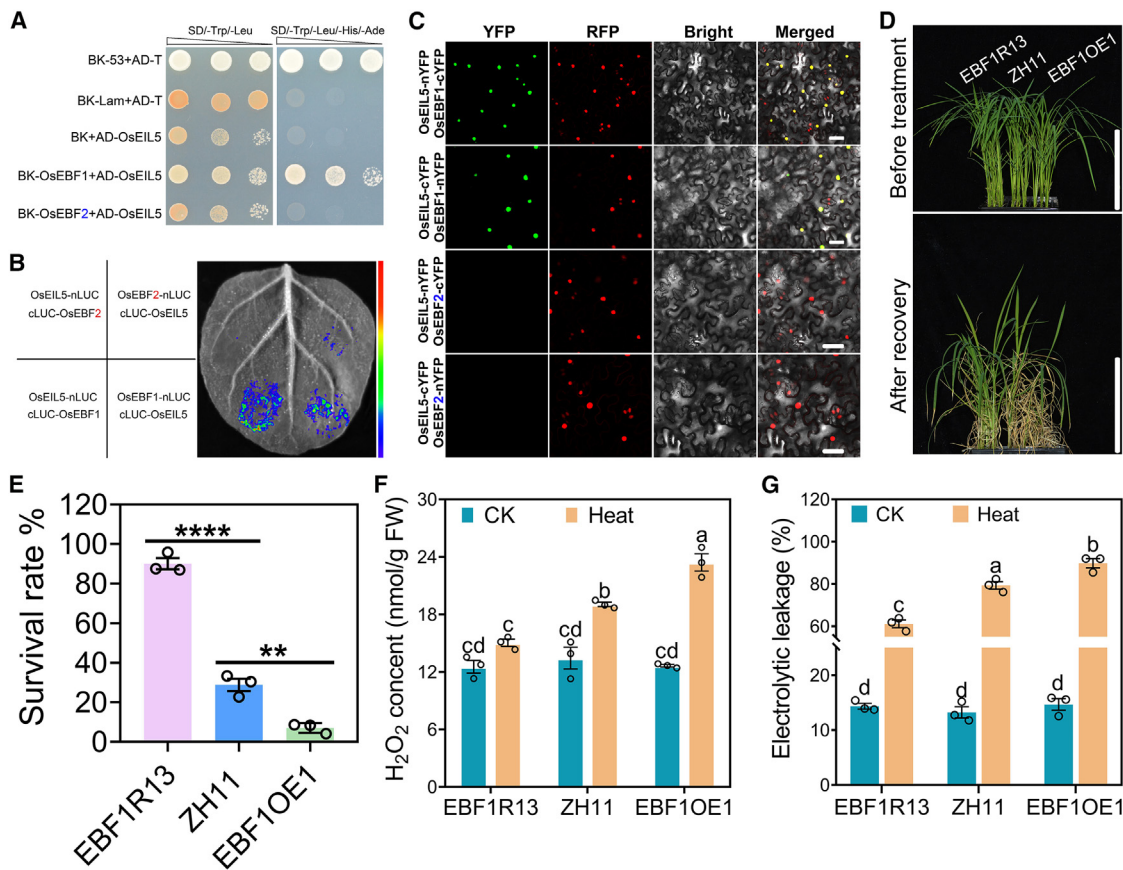


Figure 6. OsEBF1 interacts with OsEIL5 and negatively regulates heat tolerance in rice

(A) Y2H assay. BK-OsEBF1/AD-OsEIL5 or BK-OsEBF2/AD-OsEIL5 was co-transformed into yeast cells (AH109). Yeast cells co-transformed with AD-T/BK-53 or AD-T/BK-Lam vectors were used as the positive or negative control, respectively.

(B) LCI assay. Agrobacterial strains containing different combinations of plasmids were co-infiltrated into tobacco leaves. A cooled charge-coupled imaging apparatus was used to capture the images. The pseudocolor bar indicates the range of luminescence intensity.

(C) BiFC assay. Fluorescence was observed in the nuclear compartment of transformed tobacco (*N. benthamiana*) cells, resulting from the complementation of OsEIL5-nYFP+OsEBF1-cYFP or OsEIL5-cYFP+OsEBF1-nYFP. The YFP signal was detected by confocal microscopy. Scale bars: 50 μm

(D) Heat stress phenotypes of the EBF1R13 and EBF1OE1 plants. Scale bars: 12.5 cm

(E) Statistical analysis of the survival rate in (D) after heat treatment and recovery. Data represent means ± SE; n = 3 (**p < 0.01, ***p < 0.0001, Student's t test).

(F and G) H₂O₂ content (F) and electrolytic leakage (G) in EBF1R13 and EBF1OE1 before and after heat treatment. Data represent means ± SE; n = 3. Different letters above the bars indicate differences by one-way ANOVA with Tukey's multiple-comparison test at p < 0.05. See also Figures S6A and S6B.

cells. The strong YFP signal was visualized mainly from the OsEIL5-nYFP/OsEBF1-cYFP or OsEIL5-cYFP/OsEBF1-nYFP complementation assay in the nucleus of the transformed cells but not in the leaves co-expressing OsEIL5-nYFP/OsEBF2-cYFP or OsEIL5-cYFP/OsEBF2-nYFP (nYFP, N-terminal of yellow fluorescent protein; cYFP, C-terminal of yellow fluorescent protein) (Figure 6C). Taken overall, we conclude that OsEBF1 physically interacts with OsEIL5 in the nucleus.

Considering that OsEBF1 can interact with OsEIL5, we wondered whether OsEBF1 is involved in rice thermotolerance. First, we checked the response of OsEBF1 to heat stress and found that this gene was obviously inhibited at 45°C (Figure S6B). Then, we obtained one RNAi line (EBF1R13) and one OE line (EBF1OE1) of *OsEBF1*.¹⁵ When treated with 45°C for 48 h, EBF1R13 was more tolerant while EBF1OE1 was more sensitive than ZH11. The survival rates for EBF1R13, ZH11, and EBF1OE1

were 90.1%, 28.8%, and 7.1%, respectively (Figures 6D and 6E). Under heat stress, EBF1R13 accumulated less while EBF1OE1 accumulated more H₂O₂ than ZH11 (Figure 6F). Additionally, EBF1R13 had lower while EBF1OE1 had higher electrolytic leakage than ZH11 (Figure 6G). Collectively, OsEBF1 interacts with OsEIL5 and negatively modulates the thermotolerance of rice.

OsEBF1 inhibits OsPP91 expression by promoting the ubiquitination-mediated degradation of OsEIL5

Based on the fact that OsEBF1 interacts with OsEIL5, and that they regulate rice thermotolerance in an opposite manner, we tried to determine whether OsEBF1 can promote the degradation of OsEIL5 like OsEIL1.¹⁵ To examine the roles of OsEBF1 in the polyubiquitination of OsEIL5 *in vivo*, we performed ubiquitination assays in rice protoplasts. As shown in Figure 7A,

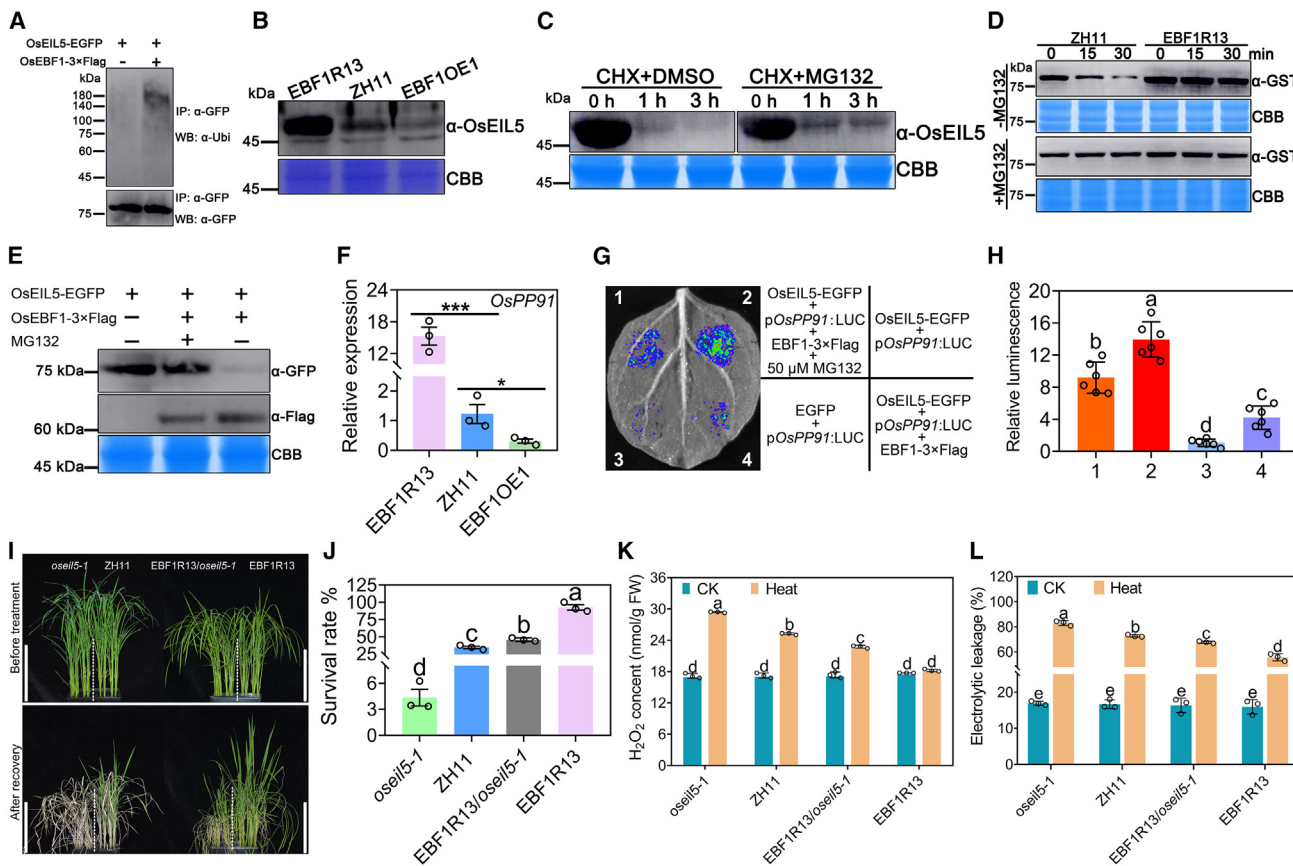


Figure 7. OsEBF1 inhibits the expression of OsPP91 by promoting the ubiquitination-mediated degradation of OsEIL5

- (A) *In vivo* ubiquitination assay. The OsEIL5-EGFP protein was immunoprecipitated using GFP-Trap from rice protoplasts expressing OsEIL5-EGFP only or co-expressing OsEIL5-EGFP and OsEBF1-3×FLAG and then subjected to western blotting using anti-Ubi (ubiquitin) and anti-GFP antibodies.
- (B) Western blot analysis of OsEIL5 levels in EBF1R13, ZH11, and EBF1OE1 plants. Total protein was extracted from seedlings under normal growth conditions, and then OsEIL5 was detected using an anti-OsEIL5 antibody.
- (C) *In vivo* OsEIL5 degradation assay. The OsEIL5-OE (OE9-3) seedlings were transferred to nutrient solution containing 300 mM CHX+DMSO or 300 mM CHX+50 μM MG132. Samples were harvested for protein extraction at the indicated time points. OsEIL5 was detected with an anti-OsEIL5 antibody.
- (D) *In vitro* cell-free OsEIL5 degradation assays. Recombinant purified GST-OsEIL5 was incubated with total protein extracted from ZH11 and EBF1R13 plants with or without 50 μM MG132. OsEIL5 was detected with an anti-GST antibody.
- (E) MG132 inhibits OsEBF1-induced OsEIL5 degradation. Different combinations of plasmids (OsEIL5-EGFP or OsEIL5-EGFP+OsEBF1-3×FLAG) were introduced into rice protoplasts. Transfected cells were cultured for 10–16 h with or without 50 μM MG132 treatment. The accumulation of OsEIL5-EGFP was analyzed using an anti-GFP antibody. The abundance of OsEBF1-3×FLAG was detected with an anti-FLAG antibody.
- (F) RT-qPCR analysis of OsPP91 expression in EBF1R13 and EBF1OE1 plants grown under normal conditions. Data represent means ± SE; n = 3 (*p < 0.05, ***p < 0.001, Student's t test).
- (G) The OsEIL5-activated OsPP91 promoter activity could be suppressed through OsEBF1. Agrobacterium strains containing different combinations of plasmids with or without MG132 were co-infiltrated into tobacco leaves. A cooled charge-coupled imaging apparatus was used to capture the images. The pseudocolor bar indicates the range of luminescence intensity.
- (H) Quantitative analysis of luminescence intensity for each image in (E).
- (I) Heat stress phenotypes of the osei5-1, ZH11, EBF1R13/osei5-1, and EBF1R13 plants. Scale bars: 12.5 cm
- (J) Statistical analysis of survival rate in (I) after heat treatment and recovery.
- (K and L) H₂O₂ content (K) and electrolytic leakage (L) in osei5-1, ZH11, EBF1R13/osei5-1, and EBF1R13 before and after heat treatment.
- In (A)–(E), the experiments were repeated three times with similar results. Coomassie brilliant blue staining was used as a loading control. In (H) and (J)–(L), data represent means ± SE; n = 6 or 3. Different letters above the bars indicate differences by one-way ANOVA with Tukey's multiple-comparisons test at p < 0.05. See also Figures S6C and S6D.

OsEBF1-3×FLAG markedly increased the polyubiquitination level of OsEIL5. To detect the endogenous OsEIL5 protein, we acquired a polyclonal antibody of this protein. After performing immunoblotting with the anti-OsEIL5 antibody, we found that OsEIL5 in OE7-1 was significantly higher than in ZH11, while

only an extremely weak OsEIL5 signal could be detected in osei5-1 (Figure S6C), which thoroughly verified the specificity of this antibody. Subsequently, we discovered that OsEIL5 in EBF1R13 was significantly higher than in ZH11 and EBF1OE1, indicating that OsEBF1 might influence the abundance of

OsEIL5 through polyubiquitination-mediated degradation (Figure 7B). When OE9-3 was treated with cycloheximide (CHX, a protein synthesis inhibitor) and MG132 (a 26S proteasome inhibitor), OsEIL5 was degraded much more slowly than in the plants treated with CHX and DMSO (mock) (Figure 7C). To further confirm whether the polyubiquitinated OsEIL5 was degraded through the 26S proteasome, we performed *in vitro* cell-free protein degradation assays. As shown in Figure 7D, without MG132, rapid degradation of OsEIL5 was observed in ZH11, but the degradation extent in EBF1R13 was significantly reduced in the same time period. The presence of MG132 stabilized GST-OsEIL5, with no visible degradation observed in either ZH11 or EBF1R13. Consistently, the abundance of OsEIL5-EGFP was extremely low in the protoplasts with additional expression of OsEBF1-3×FLAG. The reduction in OsEIL5-EGFP accumulation induced by OsEBF1-3×FLAG was suppressed by MG132 (Figure 7E). Because the mRNA levels of *OsEIL5* are not significantly different in EBF1R13, EBF1OE1, and ZH11 (Figure S6D), we deduce that OsEBF1 regulates the degradation of OsEIL5 through the ubiquitination-mediated 26S proteasome pathway.

Next, we found that EBF1R13 had higher *OsPP91* expression than ZH11, while EBF1OE1 showed the opposite trend (Figure 7F). To determine the influence of OsEBF1 on promoter activity of *OsPP91*, we once again carried out a luciferase assay. In contrast to the sole expression of p*OsPP91*:LUC, the tobacco leaves co-expressing OsEIL5-EGFP and p*OsPP91*:LUC exhibited a stronger fluorescence signal. But on this basis, after expressing OsEBF1-3×FLAG, the signals weakened rapidly, and the addition of MG132 could partially restore the signals (Figures 7G and 7H), indicating that additional expression of OsEBF1 suppressed the OsEIL5-enhanced *OsPP91* promoter activity and that ubiquitination-mediated protein degradation was involved. Together, these findings demonstrate that OsEBF1 inhibits the transcription of *OsPP91* by promoting the ubiquitination-mediated degradation of OsEIL5.

To explore the genetic interaction of OsEBF1 and OsEIL5, we produced a double-gene-modified line by crossing EBF1R13 and *oseil5-1* (EBF1R13/*oseil5-1*). When subjected to heat treatment (45°C for 48 h), *oseil5-1* was highly sensitive, and EBF1R13 exhibited extremely strong resistance. Surprisingly, although the heat tolerance of EBF1R13/*oseil5-1* was notably lower than that of EBF1R13, it was higher than that of *oseil5-1* and even higher than that of ZH11. The survival rates of *oseil5-1*, ZH11, EBF1R13/*oseil5-1*, and EBF1R13 were 4.3%, 34.4%, 45.6%, and 92.5%, respectively (Figures 7I and 7J). The magnitude order of H₂O₂ content and electrolytic leakage of the plants after heat treatment was contrary to that of the survival rates (Figures 7K and 7L). These results indicate that the functionality of OsEBF1 during rice response to heat stress is partially reliant on OsEIL5.

DISCUSSION

The EIN3/EIL master transcription factors play an amplifying role in ethylene signaling.^{7,8} There are six EIL homologs in rice (OsEIL1–OsEIL6); however, it has not been reported whether they are involved in the response to heat stress. In *Arabidopsis*, the F box proteins EBF1 and EBF2 interact with EIN3/EIL1 and

regulate their stability through a 26S proteasome degradation pathway.^{42,43} In rice, OsEBF1 physically interacts with OsEIL1 and degrades it through the 26S proteasome pathway.¹⁵ Here, we find that OsEBF1 interacts with OsEIL5 and negatively regulates rice heat tolerance by degrading OsEIL5 (Figures 6 and 7). EBF1R13, an *OsEBF1*-interfering line,¹⁵ possesses more OsEIL5 and extremely strong thermotolerance (Figures 6D–6G and 7B). Nevertheless, upon knocking out *OsEIL5* in EBF1R13, although the heat tolerance of EBF1R13/*oseil5-1* was conspicuously decreased, it did not drop to a similar level as that of *oseil5-1* and was even higher than that of ZH11 (Figures 7I–7L). This implies that the heat tolerance of EBF1R13 is only partially reliant on OsEIL5 and that there should be other target proteins that can be degraded by EBF1R13 that are also exerting their functions.

OsEIL1 and OsEIL2 have been confirmed to be involved in the ethylene signaling pathway and to be capable of regulating multiple biological processes in rice,^{10,12,15,19} but no participation in rice heat tolerance has been discovered. However, it has been demonstrated that the *Arabidopsis ein3 eil* double mutant is more susceptible to heat stress.²³ Adding 10 μM ACC can significantly enhance rice heat tolerance.⁴⁴ Accordingly, we postulate that *OsEIL1–OsEIL3*, which are also induced under high-temperature conditions, are very likely to positively regulate the heat tolerance of rice. The most likely candidate is OsEIL1 because it has been confirmed to interact with OsEBF1 and to be degraded.¹⁵ Due to the fact that the transgenic lines of *OsEIL5* have a similar sensitivity to ACC or ethephon as ZH11 (Figures S2I–S2L), OsEBF1 is anticipated to negatively modulate rice heat tolerance through ethylene-dependent and ethylene-independent mechanisms.

OsPP91 encodes a PP2C; PP2Cs are the main category of plant protein phosphatases and play important roles in response to various stresses.^{24,45–48} In this study, we found that knocking out *OsPP91*, the target of OsEIL5, significantly reduced rice heat tolerance at the seedling stage. Overexpressing *OsPP91* partially rescues thermal sensitivity of *oseil5-1* (Figure 5), indicating that *OsPP91* is a positive regulator of rice heat tolerance. *OsPP18*, a homologous protein of *OsPP91*, has dephosphorylation activity and modulates rice drought tolerance. Upon exposure to oxidative stress, the levels of H₂O₂ and electrolytic leakage in *ospp18* (drought sensitive) were significantly higher than in the wild type (WT).²⁷ Analogously, the content of H₂O₂ and electrolytic leakage in *oseil5* or *ospp91* after heat stress were also conspicuously higher than in ZH11 (Figures 1E, 1F, 5C, and 5D). Cassava MePP2C1 negatively modulates thermotolerance by fine-tuning dephosphorylation of two antioxidant enzymes, MeCAT1 and MeAPX2.³² Only when phosphorylated do they possess a strong ROS (reactive oxygen species)-scavenging capability. Distinct from MePP2C1, we conjecture that *OsPP91* positively regulates heat tolerance by dephosphorylating its interacting proteins. When these interacting proteins are phosphorylated, they might give rise to excessive accumulation of H₂O₂. For instance, when OsRbohB is phosphorylated, it can facilitate the generation of H₂O₂.⁴⁹ OsMRLK63 can phosphorylate multiple NADPH (nicotinamide adenine dinucleotide phosphate) oxidases and activate them, thereby elevating the H₂O₂ levels of plants.⁵⁰

Therefore, we believe that the physiological output of OsPP91 upregulation leading to enhanced heat tolerance is mainly due to reduced H₂O₂ production and electrolyte leakage. Further identification of the interacting proteins of OsPP91 will contribute to clarifying how it improves the heat tolerance of rice.

Due to the fact that OsPP91 only partially restored the heat sensitivity of *oseil5-1*, we are convinced that there are additional genes controlled by OsEIL5. Heat stress causes the accumulation of misfolded proteins in the ER, triggering ER stress.⁴⁰ Mutation of OsNTL3 confers heat sensitivity, while inducible expression of the truncated form of OsNTL3 increases rice heat tolerance. OsNTL3 encodes a plasma membrane-associated NAC (NAM-ATAF1/2-CUC2) transcription factor and regulates the expression of genes involved in ER protein folding.⁵¹ In our study, RNA-seq shows that multiple genes involved in protein processing in ER cannot be effectively induced by heat in *oseil5-1* (Figures S5A–S5D). Among them, Os02g0115900 and Os03g0832200, which encode an ER chaperone (BiP1) and calreticulin precursor, respectively, are also regulated by OsNTL3. The heat induction of them in *ntl3-1* is lower than in the WT.⁵¹ Additionally, we discovered that OsEIL5 positively regulates rice resistance to ER stress simulated by DTT (Figures S5E and S5F). Based on this, we speculate that, apart from OsPP91, OsEIL5 can also improve rice thermotolerance by directly activating the expression of ER stress-related genes to eliminate misfolded proteins, which is similar to the role of OsNTL3.

In summary, we proposed a possible working model for the OsEBF1-OsEIL5-OsPP91 module. In *OsEBF1-OE* plants, a large amount of OsEBF1 interacts with OsEIL5 and degrades it through ubiquitination. As a result, not enough OsEIL5 can bind to the OsPP91 promoter, leading to reduced OsPP91 transcription and greater sensitivity to high temperature. On the contrary, if the amount of OsEBF1 is limited, then most OsEIL5 cannot be degraded, so it can bind to the OsPP91 promoter and activate OsPP91 expression, thereby enhancing rice heat tolerance. The OsEBF1-OsEIL5-OsPP91 module regulates rice heat tolerance in a hierarchical manner, involving ubiquitination at the translational level and transcriptional activation at the transcriptional level.

Limitations of the study

In this research, we dissected the molecular mechanism through which the OsEBF1-OsEIL5-OsPP91 module regulates rice thermotolerance. Nevertheless, it is indispensable to accentuate certain specific constraints in our analysis. First, we are unable to ascertain whether OsEIL1, which can be degraded by OsEBF1, contributes to EBF1R13 attaining an extremely high heat tolerance. Second, the overexpression of OsEBF1 reduced the protein accumulation of OsEIL5. However, whether the overexpression of OsEIL5 on this foundation would alleviate the stronger heat sensitivity of EBF1OE1 remains unknown. Third, it is unknown whether OsPP91 possesses phosphatase activity, what its interacting proteins are, and by what means it influences heat tolerance. Finally, apart from OsPP91, although OsEIL5 affects the expression of some ER stress-related genes, it remains unclear precisely which genes are direct targets of OsEIL5 for regulating heat tolerance.

RESOURCE AVAILABILITY

Lead contact

Requests for further information, resources, and reagents should be directed to and will be fulfilled by the lead contact, Weifeng Xu (wfxu@fafu.edu.cn).

Materials availability

The plants and plasmids generated in this work can be requested from the [lead contact](#). This study did not generate new unique reagents.

Data and code availability

- The raw RNA-seq data generated in this study have been deposited in the Genome Sequence Archive in the BIG Data Center (<https://bigd.big.ac.cn>), Beijing Institute of Genomics (BIG), Chinese Academy of Sciences, and are publicly available as of the date of publication. The accession number is listed in the [key resources table](#).
- This paper does not report original code.
- Any additional information required to reanalyze the data reported in this paper is available from the [lead contact](#) upon request.

ACKNOWLEDGMENTS

We thank Prof. Xuexia Miao (Center for Excellence in Molecular Plant Sciences, Chinese Academy of Sciences) and Dr. Feilong Ma (Key Laboratory of Plant Genetics and Molecular Breeding, Zhoukou Normal University) for kindly providing the seeds of EBF1R13 and BF1OE1. This study was funded by the National Natural Science Foundation of China (grant no. 32171932), the National Scientific and Technological Innovation 2030-Major Project (grant no. 2023ZD04072), and the Natural Science Foundation of Fujian Province (grant nos. 2023J02010 and 2021J01088).

AUTHOR CONTRIBUTIONS

J.L. and W.X. designed the experiments and wrote the manuscript. J.L., K.W., G.W., Z.P., T.W., Y.M., J. Huang, J. Huo, X.L., X.Z., and H.C. conducted the experiments. J.L., K.W., and G.W. organized and analyzed the data. F.X., Q.Z., Z.W., and Y.W. contributed to the experimental design and manuscript revision. All authors have read and approved the final manuscript.

DECLARATION OF INTERESTS

The authors declare no competing interests.

STAR METHODS

Detailed methods are provided in the online version of this paper and include the following:

- [KEY RESOURCES TABLE](#)
- [EXPERIMENTAL MODEL AND STUDY PARTICIPANT DETAILS](#)
 - *Oryza sativa*
 - *Nicotiana benthamiana*
 - Bacterial strains
- [METHOD DETAILS](#)
 - Analysis of gene expression patterns
 - Thermotolerance assay
 - Expression constructs and their transformation in plants
 - RNA extraction and RT-qPCR analysis
 - Physiological parameter determination
 - Subcellular localization analysis
 - Transcriptional activation assay in yeast
 - ChIP-PCR assay
 - Biochemical assays in yeast
 - Electrophoretic mobility shift assay
 - Transactivation assay in tobacco leaves
 - ACC or ethephon treatment
 - ABA sensitivity analysis

- RNA-seq analysis
- Luciferase complementation imaging assay
- Bimolecular fluorescence complementation assay
- Detection of OsEIL5 protein level
- Analysis on the ubiquitination and degradation of OsEIL5

● QUANTIFICATION AND STATISTICAL ANALYSIS

SUPPLEMENTAL INFORMATION

Supplemental information can be found online at <https://doi.org/10.1016/j.celrep.2025.115271>.

Received: July 30, 2024

Revised: November 27, 2024

Accepted: January 15, 2025

Published: February 4, 2025

REFERENCES

1. Wang, E., Martre, P., Zhao, Z., Ewert, F., Maiorano, A., Rötter, R.P., Kimball, B.A., Ottman, M.J., Wall, G.W., White, J.W., et al. (2017). The uncertainty of crop yield projections is reduced by improved temperature response functions. *Nat. Plants* 3, 17102. <https://doi.org/10.1038/nplants.2017.102>.
2. IPCC (2021). Climate Change 2021: The Physical Science Basis. Contribution of Working Group I to the Sixth Assessment Report of the Intergovernmental Panel on Climate Change (Cambridge University Press), pp. 56–73. <https://doi.org/10.1017/9781009157896>.
3. Zhao, C., Liu, B., Piao, S., Wang, X., Lobell, D.B., Huang, Y., Huang, M., Yao, Y., Bassu, S., Ciais, P., et al. (2017). Temperature increase reduces global yields of major crops in four independent estimates. *Proc. Natl. Acad. Sci. USA* 114, 9326–9331. <https://doi.org/10.1073/pnas.1701762114>.
4. Kan, Y., and Lin, H.X. (2021). Molecular regulation and genetic control of rice thermal response. *Crop J.* 9, 497–505. <https://doi.org/10.1016/j.cj.2021.02.008>.
5. Kan, Y., Mu, X.R., Gao, J., Lin, H.X., and Lin, Y. (2023). The molecular basis of heat stress responses in plants. *Mol. Plant* 16, 1612–1634. <https://doi.org/10.1016/j.molp.2023.09.013>.
6. Li, J.Y., Yang, C., Xu, J., Lu, H.P., and Liu, J.X. (2023). The hot science in rice research: How rice plants cope with heat stress. *Plant Cell Environ.* 46, 1087–1103. <https://doi.org/10.1111/pce.14509>.
7. Zhao, H., Yin, C.C., Ma, B., Chen, S.Y., and Zhang, J.S. (2021). Ethylene signaling in rice and : New regulators and mechanisms. *J. Integr. Plant Biol.* 63, 102–125. <https://doi.org/10.1111/jipb.13028>.
8. Yang, C., Lu, X., Ma, B., Chen, S.Y., and Zhang, J.S. (2015). Ethylene Signaling in Rice and *Arabidopsis*: Conserved and Diverged Aspects. *Mol. Plant* 8, 495–505. <https://doi.org/10.1016/j.molp.2015.01.003>.
9. Mao, C., Wang, S., Jia, Q., and Wu, P. (2006). *OsEIL1*, a rice homolog of the *Arabidopsis EIN3* regulates the ethylene response as a positive component. *Plant Mol. Biol.* 61, 141–152. <https://doi.org/10.1007/s11103-005-6184-1>.
10. Yang, C., Ma, B., He, S.J., Xiong, Q., Duan, K.X., Yin, C.C., Chen, H., Lu, X., Chen, S.Y., and Zhang, J.S. (2015). *MAOHUZI6/ETHYLENE INSENSITIVE3-LIKE1* and *ETHYLENE INSENSITIVE3-LIKE2* Regulate Ethylene Response of Roots and Coleoptiles and Negatively Affect Salt Tolerance in Rice. *Plant Physiol.* 169, 148–165. <https://doi.org/10.1104/pp.15.00353>.
11. Qin, H., Zhang, Z., Wang, J., Chen, X., Wei, P., and Huang, R. (2017). The activation of *OsEIL1* on *YUC8* transcription and auxin biosynthesis is required for ethylene-inhibited root elongation in rice early seedling development. *PLoS Genet.* 13, e1006955. <https://doi.org/10.1371/journal.pgen.1006955>.
12. Yang, C., Li, W., Cao, J., Meng, F., Yu, Y., Huang, J., Jiang, L., Liu, M., Zhang, Z., Chen, X., et al. (2017). Activation of ethylene signaling pathways enhances disease resistance by regulating ROS and phytoalexin production in rice. *Plant J.* 89, 338–353. <https://doi.org/10.1111/tpj.13388>.
13. Zhao, Y., Zhu, X., Shi, C.M., Xu, G., Zuo, S., Shi, Y., Cao, W., Kang, H., Liu, W., Wang, R., et al. (2024). *OsEIL2* balances rice immune responses against (hemi) biotrophic and necrotrophic pathogens via the salicylic acid and jasmonic acid synergism. *New Phytol.* 243, 362–380. <https://doi.org/10.1111/nph.19809>.
14. Zhu, X., Zhao, Y., Shi, C.M., Xu, G., Wang, N., Zuo, S., Ning, Y., Kang, H., Liu, W., Wang, R., et al. (2024). Antagonistic control of rice immunity against distinct pathogens by the two transcription modules via salicylic acid and jasmonic acid pathways. *Dev. Cell* 59, 1609–1622.e4. <https://doi.org/10.1016/j.devcel.2024.03.033>.
15. Ma, F., Yang, X., Shi, Z., and Miao, X. (2020). Novel crosstalk between ethylene- and jasmonic acid-pathway responses to a piercing-sucking insect in rice. *New Phytol.* 225, 474–487. <https://doi.org/10.1111/nph.16111>.
16. Wei, Y., Zhu, B., Ma, G., Shao, X., Xie, H., Cheng, X., Zeng, H., and Shi, H. (2022). The coordination of melatonin and anti-bacterial activity by EIL5 underlies ethylene-induced disease resistance in cassava. *Plant J.* 111, 683–697. <https://doi.org/10.1111/tpj.15843>.
17. Lei, G., Shen, M., Li, Z.G., Zhang, B., Duan, K.X., Wang, N., Cao, Y.R., Zhang, W.K., Ma, B., Ling, H.Q., et al. (2011). *EIN2* regulates salt stress response and interacts with a MA3 domain-containing protein ECIP1 in *Arabidopsis*. *Plant Cell Environ.* 34, 1678–1692. <https://doi.org/10.1111/j.1365-3040.2011.02363.x>.
18. Peng, J., Li, Z., Wen, X., Li, W., Shi, H., Yang, L., Zhu, H., and Guo, H. (2014). Salt-Induced Stabilization of *EIN3/EIL1* Confers Salinity Tolerance by Deterring ROS Accumulation in *Arabidopsis*. *PLoS Genet.* 10, e1004664. <https://doi.org/10.1371/journal.pgen.1004664>.
19. Zhai, M., Chen, Y., Pan, X., Chen, Y., Zhou, J., Jiang, X., Zhang, Z., Xiao, G., and Zhang, H. (2024). *OsEIN2-OsEIL1/2* pathway negatively regulates chilling tolerance by attenuating *OsICE1* function in rice. *Plant Cell Environ.* 47, 2561–2577. <https://doi.org/10.1111/pce.14900>.
20. Li, G., Zhang, L., Wu, J., Yue, X., Wang, M., Sun, L., Di, D., Kronzucker, H.J., and Shi, W. (2022). *OsEIL1* protects rice growth under NH_4^+ nutrition by regulating *OsVTC1-3*-dependent N-glycosylation and root NH_4^+ efflux. *Plant Cell Environ.* 45, 1537–1553. <https://doi.org/10.1111/pce.14283>.
21. Larkindale, J., Hall, J.D., Knight, M.R., and Vierling, E. (2005). Heat stress phenotypes of arabidopsis mutants implicate multiple signaling pathways in the acquisition of thermotolerance. *Plant Physiol.* 138, 882–897. <https://doi.org/10.1104/pp.105.062257>.
22. Larkindale, J., and Knight, M.R. (2002). Protection against heat stress-induced oxidative damage in arabidopsis involves calcium, abscisic acid, ethylene, and salicylic acid. *Plant Physiol.* 128, 682–695. <https://doi.org/10.1104/pp.010320>.
23. Huang, J., Zhao, X., Bürger, M., Wang, Y., and Chory, J. (2021). Two interacting ethylene response factors regulate heat stress response. *Plant Cell* 33, 338–357. <https://doi.org/10.1093/plcell/koaa026>.
24. Singh, A., Jha, S.K., Bagri, J., and Pandey, G.K. (2015). ABA Inducible Rice Protein Phosphatase 2C Confers ABA Insensitivity and Abiotic Stress Tolerance in *Arabidopsis*. *PLoS One* 10, e0125168. <https://doi.org/10.1371/journal.pone.0125168>.
25. Miao, J., Li, X., Li, X., Tan, W., You, A., Wu, S., Tao, Y., Chen, C., Wang, J., Zhang, D., et al. (2020). *OsPP2C09*, a negative regulatory factor in abscisic acid signalling, plays an essential role in balancing plant growth and drought tolerance in rice. *New Phytol.* 227, 1417–1433. <https://doi.org/10.1111/nph.16670>.
26. Min, M.K., Kim, R., Hong, W.J., Jung, K.H., Lee, J.Y., and Kim, B.G. (2021). *OsPP2C09* Is a Bifunctional Regulator in Both ABA-Dependent and Independent Abiotic Stress Signaling Pathways. *Int. J. Mol. Sci.* 22, 393. <https://doi.org/10.3390/ijms22010393>.

27. You, J., Zong, W., Hu, H., Li, X., Xiao, J., and Xiong, L. (2014). A STRESS-RESPONSIVE NAC1-Regulated Protein Phosphatase Gene Rice Modulates Drought and Oxidative Stress Tolerance through Abscisic Acid-Independent Reactive Oxygen Species Scavenging in Rice. *Plant Physiol.* 166, 2100–2114. <https://doi.org/10.1104/pp.114.251116>.
28. Hu, X., Zhang, H., Li, G., Yang, Y., Zheng, Z., and Song, F. (2009). Ectopic expression of a rice protein phosphatase 2C gene *OsB1PP2C2* in tobacco improves disease resistance. *Plant Cell Rep.* 28, 985–995. <https://doi.org/10.1007/s00299-009-0701-7>.
29. Park, C.J., Peng, Y., Chen, X.W., Dardick, C., Ruan, D.L., Bart, R., Canlas, P.E., and Ronald, P.C. (2008). Rice XB15, a Protein Phosphatase 2C, Negatively Regulates Cell Death and XA21-Mediated Innate Immunity. *PLoS Biol.* 6, 2614. <https://doi.org/10.1371/journal.pbio.0060282>.
30. Liu, Q., Ding, J., Huang, W., Yu, H., Wu, S., Li, W., Mao, X., Chen, W., Xing, J., Li, C., and Yan, S. (2022). OsPP65 Negatively Regulates Osmotic and Salt Stress Responses Through Regulating Phytohormone and Raffinose Family Oligosaccharide Metabolic Pathways in Rice. *Rice* 15, 34. <https://doi.org/10.1186/s12284-022-00581-5>.
31. Xie, W., Liu, S., Gao, H., Wu, J., Liu, D., Kinoshita, T., and Huang, C.F. (2023). PP2C.D phosphatase SAL1 positively regulates aluminum resistance via restriction of aluminum uptake in rice. *Plant Physiol.* 192, 1498–1516. <https://doi.org/10.1093/plphys/kiad122>.
32. Bai, Y., Dong, Y., Zheng, L., Zeng, H., Wei, Y., and Shi, H. (2024). Cassava phosphatase PP2C1 modulates thermotolerance via fine-tuning dephosphorylation of antioxidant enzymes. *Plant Physiol.* 194, 2724–2738. <https://doi.org/10.1093/plphys/kiae009>.
33. Ma, X., Zhang, Q., Zhu, Q., Liu, W., Chen, Y., Qiu, R., Wang, B., Yang, Z., Li, H., Lin, Y., et al. (2015). A Robust CRISPR/Cas9 System for Convenient, High-Efficiency Multiplex Genome Editing in Monocot and Dicot Plants. *Mol. Plant* 8, 1274–1284. <https://doi.org/10.1016/j.molp.2015.04.007>.
34. Endo, M., Tsuchiya, T., Hamada, K., Kawamura, S., Yano, K., Ohshima, M., Higashitani, A., Watanabe, M., and Kawagishi-Kobayashi, M. (2009). High Temperatures Cause Male Sterility in Rice Plants with Transcriptional Alterations During Pollen Development. *Plant Cell Physiol.* 50, 1911–1922. <https://doi.org/10.1093/pcp/pcp135>.
35. Martin, K., Kopperud, K., Chakrabarty, R., Banerjee, R., Brooks, R., and Goodin, M.M. (2009). Transient expression in fluorescent marker lines provides enhanced definition of protein localization, movement and interactions. *Plant J.* 59, 150–162. <https://doi.org/10.1111/j.1365-313X.2009.03850.x>.
36. Zhang, B., Zhu, X., Chen, Z., Zhang, H., Huang, J., and Huang, J. (2023). RiceTTarget: A rice transcription factor-target prediction server based on coexpression and machine learning. *Plant Physiol.* 193, 190–194. <https://doi.org/10.1093/plphys/kiad332>.
37. Li, P., Lei, K., Li, Y., He, X., Wang, S., Liu, R., Ji, L., and Hou, B. (2019b). Identification and characterization of the first cytokinin glycosyltransferase from rice. *Rice* 12, 19. <https://doi.org/10.1186/s12284-019-0279-9>.
38. Li, Y., Liu, F., Li, P., Wang, T., Zheng, C., and Hou, B. (2020). An Cytokinin-Modifying Glycosyltransferase UGT76C2 Improves Drought and Salt Tolerance in Rice. *Front. Plant Sci.* 11, 560696. <https://doi.org/10.3389/fpls.2020.560696>.
39. Hubbard, K.E., Nishimura, N., Hitomi, K., Getzoff, E.D., and Schroeder, J.I. (2010). Early abscisic acid signal transduction mechanisms: newly discovered components and newly emerging questions. *Gene Dev.* 24, 1695–1708. <https://doi.org/10.1101/gad.1953910>.
40. Liu, J.X., and Howell, S.H. (2010). Endoplasmic Reticulum Protein Quality Control and Its Relationship to Environmental Stress Responses in Plants. *Plant Cell* 22, 2930–2942. <https://doi.org/10.1101/tpc.110.078154>.
41. Ma, F., Li, Z., Wang, S., Li, K., Tang, F., Jia, J., Zhao, Q., Jing, P., Yang, W., Hua, C., et al. (2023). The F-box protein OsEBF2 confers the resistance to the brown planthopper (*Nilparvata lugens* Stål). *Plant Sci.* 327, 111547. <https://doi.org/10.1016/j.plantsci.2022.111547>.
42. Guo, H., and Ecker, J.R. (2003). Plant responses to ethylene gas are mediated by SCF^{EBF1/EBF2}-dependent proteolysis of EIN3 transcription factor. *Cell* 115, 667–677. [https://doi.org/10.1016/S0092-8674\(03\)00969-3](https://doi.org/10.1016/S0092-8674(03)00969-3).
43. Gagne, J.M., Smalle, J., Gingerich, D.J., Walker, J.M., Yoo, S.D., Yanagisawa, S., and Vierstra, R.D. (2004). EIN3-binding F-box 1 and 2 form ubiquitin-protein ligases that repress ethylene action and promote growth by directing EIN3 degradation. *Proc. Natl. Acad. Sci. USA* 101, 6803–6808. <https://doi.org/10.1073/pnas.0401698101>.
44. Wu, Y.S., and Yang, C.Y. (2019). Ethylene-mediated signaling confers thermotolerance and regulates transcript levels of heat shock factors in rice seedlings under heat stress. *Bot. Stud.* 60, 23. <https://doi.org/10.1186/s40529-019-0272-z>.
45. Fujii, S., and Toriyama, K. (2008). DCW11, Down-Regulated Gene 11 in CW-type cytoplasmic male sterile rice, encoding mitochondrial protein phosphatase 2C is related to cytoplasmic male sterility. *Plant Cell Physiol.* 49, 633–640. <https://doi.org/10.1093/pcp/pcn072>.
46. Singh, A., Giri, J., Kapoor, S., Tyagi, A.K., and Pandey, G.K. (2010). Protein phosphatase complement in rice: genome-wide identification and transcriptional analysis under abiotic stress conditions and reproductive development. *BMC Genom.* 11, 435. <https://doi.org/10.1186/1471-2164-11-435>.
47. Fuchs, S., Grill, E., Meskiene, I., and Schweighofer, A. (2013). Type 2C protein phosphatases in plants. *FEBS J.* 280, 681–693. <https://doi.org/10.1111/j.1742-4658.2012.08670.x>.
48. Ni, L., Fu, X., Zhang, H., Li, X., Cai, X., Zhang, P., Liu, L., Wang, Q.W., Sun, M., Wang, Q., et al. (2019). Abscisic Acid Inhibits Rice Protein Phosphatase PP45 via H₂O₂ and Relieves Repression of the Ca²⁺/CaM-Dependent Protein Kinase DMI3. *Plant Cell* 31, 128–152. <https://doi.org/10.1105/tpc.18.00506>.
49. Wang, Q., Shen, T., Ni, L., Chen, C., Jiang, J., Cui, Z., Wang, S., Xu, F., Yan, R., and Jiang, M. (2023). Phosphorylation of OsRbohB by the protein kinase OsDMI3 promotes H₂O₂ production to potentiate ABA responses in rice. *Mol. Plant* 16, 882–902. <https://doi.org/10.1016/j.molp.2023.04.003>.
50. Jing, X.Q., Shi, P.T., Zhang, R., Zhou, M.R., Shalmani, A., Wang, G.F., Liu, W.T., Li, W.Q., and Chen, K.M. (2024). Rice kinase OsMRLK63 contributes to drought tolerance by regulating reactive oxygen species production. *Plant Physiol.* 194, 2679–2696. <https://doi.org/10.1093/plphys/kiad684>.
51. Liu, X.H., Lyu, Y.S., Yang, W., Yang, Z.T., Lu, S.J., and Liu, J.X. (2020). A membrane-associated NAC transcription factor OsNTL3 is involved in thermotolerance in rice. *Plant Biotechnol. J.* 18, 1317–1329. <https://doi.org/10.1111/pbi.13297>.
52. Weng, X., Wang, L., Wang, J., Hu, Y., Du, H., Xu, C., Xing, Y., Li, X., Xiao, J., and Zhang, Q. (2014). Is a Central Regulator of Growth, Development, and Stress Response. *Plant Physiol.* 164, 735–747. <https://doi.org/10.1104/pp.113.231308>.
53. Xu, Y., Zhang, L., Ou, S., Wang, R., Wang, Y., Chu, C., and Yao, S. (2020). Natural variations of SLG1 confer high-temperature tolerance in rice. *Nat. Commun.* 11, 5441. <https://doi.org/10.1038/s41467-020-19320-9>.
54. Liu, J., Zhang, C., Wei, C., Liu, X., Wang, M., Yu, F., Xie, Q., and Tu, J. (2016). The RING Finger Ubiquitin E3 Ligase OsHTAS Enhances Heat Tolerance by Promoting H₂O₂-Induced Stomatal Closure in Rice. *Plant Physiol.* 170, 429–443. <https://doi.org/10.1104/pp.15.00879>.
55. Livak, K.J., and Schmittgen, T.D. (2001). Analysis of relative gene expression data using real-time quantitative PCR and the 2^{-ddCT} Method. *Methods* 25, 402–408. <https://doi.org/10.1006/meth.2001.1262>.
56. Liu, J., Liao, W., Nie, B., Zhang, J., and Xu, W. (2021). OsUEV1B, an Ubc enzyme variant protein, is required for phosphate homeostasis in rice. *Plant J.* 106, 706–719. <https://doi.org/10.1111/tpj.15193>.
57. Yoo, S.D., Cho, Y.H., and Sheen, J. (2007). *Arabidopsis* mesophyll protoplasts: a versatile cell system for transient gene expression analysis. *Nat. Protoc.* 2, 1565–1572. <https://doi.org/10.1038/nprot.2007.199>.
58. Trapnell, C., Roberts, A., Goff, L., Pertea, G., Kim, D., Kelley, D.R., Pimentel, H., Salzberg, S.L., Rinn, J.L., and Pachter, L. (2012). Differential gene and transcript expression analysis of RNA-seq experiments with TopHat

- and Cufflinks. *Nat. Protoc.* 7, 562–578. <https://doi.org/10.1038/nprot.2012.016>.
59. Li, B., and Dewey, C.N. (2011). RSEM: accurate transcript quantification from RNA-Seq data with or without a reference genome. *BMC Bioinf.* 12, 323.
60. Anders, S., and Huber, W. (2010). Differential expression analysis for sequence count data. *Genome Biol.* 11, R106. <https://doi.org/10.1186/gb-2010-11-10-r106>.
61. Robinson, M.D., McCarthy, D.J., and Smyth, G.K. (2010). edgeR: a Bioconductor package for differential expression analysis of digital gene expression data. *Bioinformatics* 26, 139–140. <https://doi.org/10.1093/bioinformatics/btp616>.
62. Li, N., Lin, B., Wang, H., Li, X., Yang, F., Ding, X., Yan, J., and Chu, Z. (2019). Natural variation *ZmFBL41* in confers banded leaf and sheath blight resistance in maize. *Nat. Genet.* 51, 1540–1548. <https://doi.org/10.1038/s41588-019-0503-y>.
63. Sheen, J. (2001). Signal transduction in maize and *Arabidopsis* mesophyll protoplasts. *Plant Physiol.* 127, 1466–1475. <https://doi.org/10.1104/pp.010820>.

STAR★METHODS

KEY RESOURCES TABLE

| REAGENT or RESOURCE | SOURCE | IDENTIFIER |
|--|----------------|---------------------------------|
| Antibodies | | |
| Rabbit anti-OsEIL5 | This paper | N/A |
| Mouse monoclonal anti-Ubi | Millipore | Cat#05-944; RRID:AB_441944 |
| Mouse monoclonal anti-GFP | TransGen | Cat# HT801-01 |
| Mouse monoclonal anti-GST | TransGen | Cat# HT601-01 |
| Mouse monoclonal anti-Flag | TransGen | Cat# HT201-01 |
| Mouse monoclonal anti-IgG | Abcam | Cat# ab124055; RRID:AB_10949474 |
| Goat Anti-Rabbit IgG (H + L) | LABLEAD | Cat# Y1067 |
| Goat Anti-Mouse IgG (H + L) | LABLEAD | Cat# Y1106 |
| Bacterial and virus strains | | |
| <i>Escherichia coli</i> strain DH5 α | Tsingke | Cat# TSC-C01 |
| <i>Escherichia coli</i> strain BL21(DE3) | Tsingke | Cat# TSC-E01 |
| <i>Agrobacterium tumefaciens</i> GV3101(pSoup-p19) | Weidi | Cat# AC1003 |
| <i>Saccharomyces cerevisiae</i> AH109 | Weidi | Cat# YC1010 |
| <i>Saccharomyces cerevisiae</i> Y187 | Weidi | Cat# YC1020 |
| Chemicals, peptides, and recombinant proteins | | |
| MG-132 | MCE | Cat# HY-13259 |
| T4 DNA Ligase | Vazyme | Cat# C301-01 |
| KOD-Plus-Neo | Toyobo | Cat# 256400 |
| 1-Aminocyclopropanecarboxylic Acid (ACC) | Coolaber | Cat# 22059-21-8 |
| Ethepron | Sangon | Cat# A600453-0500 |
| Abscisic acid (ABA) | Sangon | Cat# A600001-0100 |
| Protease Inhibitor Cocktail, EDTA free | Roche | Cat# 04693159001 |
| TRIzol TM | Invitrogen | Cat# 15596018 |
| ChamQ SYBR qPCR Master Mix | Vazyme | Cat# Q311-03 |
| HiScript II Q RT SuperMix for qPCR (+gDNA wiper) | Vazyme | Cat# R223-01 |
| Cycloheximide (CHX) | Cell Signaling | Cat# 2112 |
| SD/-Trp/-Leu with Agar | Coolaber | Cat# PM2222 |
| SD/-Trp/-Leu/-His/-Ade with Agar | Coolaber | Cat# PM2112 |
| SD/-Trp/-Leu/-His Broth | Coolaber | Cat# PM2151 |
| 3-Amino-1,2,4-triazole (3-AT) | Coolaber | Cat# CA1311-25g |
| Dithiothreitol (DTT) | Sangon | Cat# A620058-0025 |
| Dimethyl sulfoxide (DMSO) | Sangon | Cat# A600163-0250 |
| GFP-Trap beads | ChromoTek | Cat# GTA-20 |
| Anti-Flag beads | Sigma | Cat# M8823 |
| Cellulase R10 | Yakult | Cat# 180612-02 |
| Maerozyme R10 | Yakult | Cat# 171208-02 |
| GST-OsEIL5 | This paper | N/A |
| GLUTATHIONE Sepharose 4B | GE | Cat# 17075601 |
| D-Luciferin, Potassium Salt | YEASEN | Cat# 40902ES03 |
| Protein A-agarose/Salmon Sperm DNA | Sigma-Aldrich | Cat# 16-157 |
| Critical commercial assays | | |
| ClonExpress II One Step Cloning Kit | Vazyme | Cat# C112-02 |
| LightShift Chemiluminescent EMSA Kit | Thermo Fisher | Cat# 20148 |

(Continued on next page)

Continued

| REAGENT or RESOURCE | SOURCE | IDENTIFIER |
|---|-----------------------------|----------------|
| Easy Plasmid Miniprep Kit | Easy-Do | Cat# DR0201050 |
| Easy Gel Extraction&Clean-up Kit | Easy-Do | Cat# DR0101050 |
| Matchmaker One-Hybrid System | Clontech | Cat# K1603-1 |
| Deposited data | | |
| RNA-seq data | This paper | GSA: CRA018070 |
| Experimental models: Organisms/strains | | |
| <i>Oryza Sativa</i> : Zhonghua 11 (ZH11) | This paper | N/A |
| <i>Oryza Sativa</i> : OsEIL5-OE and oseil5 | This paper | N/A |
| <i>Oryza Sativa</i> : ospp91 | This paper | N/A |
| <i>Oryza Sativa</i> : oseil5/OsPP91-OE | This paper | N/A |
| <i>Oryza Sativa</i> : EBF1R13 and EBF1OE1 | Ma et al. ¹⁵ | N/A |
| <i>Oryza Sativa</i> : EBF1R13/oseil5-1 | This paper | N/A |
| <i>Nicotiana benthamiana</i> | This paper | N/A |
| <i>Nicotiana benthamiana</i> (expressing RFP-H2B) | Martin et al. ³⁵ | N/A |
| Oligonucleotides | | |
| See Table S3 | This paper | N/A |
| Recombinant DNA | | |
| <i>Ubi:OsEIL5</i> | This paper | N/A |
| <i>Ubi:OsEIL5-3×Flag</i> | This paper | N/A |
| <i>Ubi:OsPP91</i> | This paper | N/A |
| <i>35S:OsEBF1-3×Flag</i> | This paper | N/A |
| <i>35S:OsEIL5-nYFP</i> | This paper | N/A |
| <i>35S:OsEIL5-cYFP</i> | This paper | N/A |
| <i>35S:OsEBF1-nYFP</i> | This paper | N/A |
| <i>35S:OsEBF1-cYFP</i> | This paper | N/A |
| <i>35S:OsEBF2-nYFP</i> | This paper | N/A |
| <i>35S:OsEBF2-cYFP</i> | This paper | N/A |
| <i>35S:OsEIL5-nLUC</i> | This paper | N/A |
| <i>35S:cLUC-OsEIL5</i> | This paper | N/A |
| <i>35S:OsEBF1-nLUC</i> | This paper | N/A |
| <i>35S:cLUC-OsEBF1</i> | This paper | N/A |
| <i>35S:OsEBF2-nLUC</i> | This paper | N/A |
| <i>35S:cLUC-OsEBF2</i> | This paper | N/A |
| <i>35S:OsEIL5-EGFP</i> | This paper | N/A |
| <i>35S:OsEIL5-GFP</i> | This paper | N/A |
| <i>GST-OsEIL5</i> | This paper | N/A |
| <i>proOsPP91:LUC</i> | This paper | N/A |
| <i>pHis2-proOsPP91</i> | This paper | N/A |
| <i>pGBK7-OsEIL5</i> | This paper | N/A |
| <i>pGBK7-OsEIL5(N)</i> | This paper | N/A |
| <i>pGBK7-OsEIL5(M)</i> | This paper | N/A |
| <i>pGBK7-OsEIL5(C)</i> | This paper | N/A |
| <i>pGBK7-OsEIL5(NM)</i> | This paper | N/A |
| <i>pGBK7-OsEIL5(MC)</i> | This paper | N/A |
| <i>pGADT7-OsEIL5</i> | This paper | N/A |
| <i>pGBK7-OsEBF1</i> | This paper | N/A |
| <i>pGBK7-OsEBF2</i> | This paper | N/A |
| <i>35S:OsGhd7-RFP</i> | Weng et al. ⁵² | N/A |

(Continued on next page)

Continued

| REAGENT or RESOURCE | SOURCE | IDENTIFIER |
|-------------------------|-------------------|---|
| Software and algorithms | | |
| GraphPad Prism 9.0 | GraphPad Software | https://www.graphpad.com/ |
| ImageJ | NIH | https://imagej.nih.gov/ij/ |

EXPERIMENTAL MODEL AND STUDY PARTICIPANT DETAILS

Oryza sativa

The *osil5* and *ospp91* CRISPR/Cas9 mutants, as well as the *OsEIL5*-OE and *OsEIL5*-3×Flag transgenic plants, were generated in the background of *Oryza sativa* ssp. *japonica* cv. Zhonghua11 (ZH11). The *OsEBF1*-RNAi and -OE lines in the background of ZH11 were kindly provided by Prof. Xuexia Miao (Center for Excellence in Molecular Plant Sciences, China Academy of Sciences) and Dr. Feilong Ma (Key Laboratory of Plant Genetics and Molecular Breeding, Zhoukou Normal University). The *oseil5*-1/*OsPP91*-OE transgenic lines were obtained from the overexpression of *OsPP91* in *oseil5*-1. The EBF1R13/*oseil5*-1 transgenic line was generated by crossing EBF1R13 and *oseil5*-1.

Nicotiana benthamiana

N. benthamiana plants were cultivated in soil under a 12-h light/12-h dark photoperiod at 25°C. Five-week-old *N. benthamiana* leaves were used in luciferase complementation imaging and bimolecular fluorescence complementation assays.

Bacterial strains

Agrobacterium tumefaciens GV3101 (pSoup-p19) harboring various indicated constructs was grown on LB agar media at 28°C with antibiotics. The concentration of antibiotics for agar- 25 µg mL⁻¹ rifampicin, 10 µg mL⁻¹ gentamycin, 100 µg mL⁻¹ kanamycin. The concentration of antibiotics for broth- 10 µg mL⁻¹ gentamycin, 50 µg mL⁻¹ kanamycin.

METHOD DETAILS

Analysis of gene expression patterns

To check the expression of *OsEILs* or *OsEBF1* under heat stress treatment, ZH11 plants were grown in Kimura B nutrient solution under normal conditions. The seedlings at 2.5- to 3.5-leaf stage were treated with heat stress (exposing plants to 45°C), followed by sampling at the designated times. Roots were harvested for RNA extraction and subsequent gene expression analysis. To check the expression *OsEIL5* under various abiotic stresses or phytohormone treatment, the seedlings described above were treated with ACC (50 µM), 120 mM NaCl, 20% PEG 4000, 100 mM ABA, cold (4°C), and heat (45°C), followed by sampling at 9 h after treatment. Roots were harvested for RNA extraction and subsequent gene expression analysis. The primers used are listed in Table S3.

Thermotolerance assay

For high-temperature treatment at the seedling stage, the healthy seeds were surface-sterilized with 3% sodium hypochlorite for 25 min, soaked at 35°C for 3 d. Germinating seeds were sowed into black 96-well plates without bottoms, and then each plate was placed on a black box filled with Kimura B nutrient solution, which was then cultured in the growth chamber (SAIFU) with 14 h light (28°C)/10 h dark (28°C), 65–70% relative humidity, and 150 µmol m⁻² s⁻¹ photon flux density. In another same growth chamber, the seedlings at the 3.5- to 4.5-leaf stage were treated at 45°C for a given time (other growth conditions remained the same), and then recovered under normal conditions for 7 d. The survival rate was calculated as the ratio of the number of seedlings with new green leaves to the total number of treated seedlings.

Heat stress treatment at the reproductive stage was performed as previously described with some modifications.⁵³ Germinating seeds were sowed on April 20, April 30, and May 10, respectively, and the seedlings of 5.5-leaf stage were transplanted into pots (22 cm × 22 cm × 34 cm) filled with the same amount of paddy soil, each pot with three plants, and cultivated under natural growth conditions. The tillers at the microsporocyte meiosis stage were tagged and transferred into the phytotron (PERCIVAL), with the photon flux density of 500 µmol m⁻² s⁻¹ and relative humidity of 75–80%. High-temperature treatment was performed under 40°C during the day (07:00–19:00) and 31 °C at night (19:00–07:00) for 7 d, respectively, and the plants were then recovered under normal growth conditions until seed maturation. Seed-setting rate was calculated as the percentage of the number of filled grains to the number of total spikelet in a panicle.

Expression constructs and their transformation in plants

The cDNA fragments of *OsEIL5* (1515 bp) or *OsPP91* (984 bp) were cloned into the modified pCAMBIA1300 vector (target gene driven by the maize *ubiquitin* promoter) to generate overexpression constructs with or without 3×FLAG tag. The guide RNA constructs used for CRISPR/Cas9-mediated knockout of *OsEIL5* or *OsPP91* were generated as described previously.³³ The resulting constructs were

transformed into ZH11 or *oseil5-1* mutant by *Agrobacterium*-mediated transformation. The transformants were screened by PCR amplification using primers specific for the hygromycin phosphotransferase (*HPT*) gene.⁵⁴ The primers used are listed in [Table S3](#).

RNA extraction and RT-qPCR analysis

RNA extraction and RT-qPCR analysis were performed as previously described.⁵⁴ Briefly, fresh plant tissues were harvested and immediately ground into a fine powder in liquid nitrogen. Total RNA was extracted using TRIzol reagent (Invitrogen) according to the manufacturer's instructions. The DNase-treated RNA was reverse transcribed using HiScript II Q RT SuperMix for qPCR according to the manufacturer's instructions. RT-qPCR was performed in an optical 96-well plate using ChamQ SYBR qPCR Master Mix and the CFX96 Real-Time PCR Detection System (Bio-Rad). The PCR thermal cycling protocol was 95°C for 10 s, followed by 40 cycles at 95°C for 5 s and 60°C for 30 s. *OsActin1* gene was used as the internal reference, and data analyses were performed using the 2^{-ddCt} method as described previously.⁵⁵

Physiological parameter determination

The H₂O₂ contents were measured as described previously.⁵⁴ Briefly, shoots harvested from 3.5- to 4.5-leaf stage seedlings, with or without heat treatment for 12 h, were used to measure H₂O₂ contents. The contents were measured spectrophotometrically after reaction with potassium iodide. The reaction mixture consisted of 0.5 mL of 0.1% (w/v) TCA, leaf extract supernatant, 0.5 mL of 100 mM potassium phosphate buffer (pH 7.8), and 1 mL of reagent (1 M [w/v] potassium iodide in fresh double distilled water). The blank control consisted of 1 mL of 0.1% (w/v) TCA and 1 mL of potassium iodide in the absence of leaf extract. After 1 h of reaction in darkness, the absorbance was measured at 390 nm. The amount of H₂O₂ was calculated using a standard curve prepared with known concentrations of H₂O₂.

The electrolytic leakage assay was performed as described previously.⁵¹ Briefly, rice (3.5- to 4.5-leaf stage) leaves with or without heat treatment for 6 h were placed in 20 mL of deionized water in a beaker for 2 h at room temperature, and the initial conductivity (R1) was recorded using a microprocessor-based conductivity meter. The beaker was then placed on electromagnetic oven for boiling for 10 min to release all the electrolytes into the solution, cooled to room temperature and the final conductivity (R2) was recorded. The electrolytic leakage was calculated as the ratio of conductivity before boiling to that after boiling (R1/R2).

Subcellular localization analysis

Subcellular localization assay was performed as described previously.⁵⁶ Briefly, the cDNA fragments of the target gene were amplified by PCR and directionally inserted into pCAMBIA1300-35S:EGFP and/or the transient expression vector pM999-35S:GFP. Cultures of the *Agrobacterium* strain GV3101 harboring the pCAMBIA1300-35S:EGFP constructs were used to infect the healthy leaves of tobacco (*N. benthamiana*, 4 weeks old) expressing 35S:RFP-histone 2B (nuclear marker).³⁵ The constructs of the pM999 series were transferred into rice protoplasts using the procedures described by Yoo et al.⁵⁷ Fluorescent signals were observed using a confocal microscope (Leica TCS SP5). The primers used are listed in [Table S3](#).

Transcriptional activation assay in yeast

For transcriptional activation activity assay in yeast, various truncated forms of OsEIL5 were inserted into pGBT7. Different recombinant plasmids and empty pGADT7 vector were co-transferred to yeast strain AH109 and cultured on selective plates at 30°C for 3–5 d. Transcriptional activation activity was evaluated based on the activation of the histidine (His) and adenine (Ade) reporters. The primers used are listed in [Table S3](#).

ChIP-PCR assay

For ChIP assays, the OsEIL5-3×Flag transgenic plants were used for chromatin extraction and immunoprecipitation as described previously.²⁷ Briefly, the aerial parts of three leaf-stage rice seedling were treated with formaldehyde, and the nuclei were isolated and sonicated using an Ultrasonic Crasher Noise Isolating Chamber (SCIENTZ). The soluble chromatin fragments were isolated and preabsorbed with sheared salmon sperm DNA/protein A-agarose to remove nonspecific binding. Immunoprecipitations with anti-Flag antibody and anti-IgG antibody were prepared as described. The precipitated DNA was analyzed by PCR using specific primer sets ([Table S3](#)). Typically, 26 to 28 cycles were performed for the PCR.

Biochemical assays in yeast

Yeast one-hybrid (Y1H) assay was performed using the Matchmaker One-Hybrid System (Clontech). The OsPP91 promoter fragment (−13 to −895 bp upstream of ATG) was fused upstream to the HIS3 minimal promoter and served as a reporter construct. OsEIL5 was fused to the Gal4 activation domain in the pGADT7 vector (AD-OsEIL5) and co-transformed with the reporter vector (pHis2-pOsPP18) into Y187 yeast cells for determination of the DNA-protein interactions.

Yeast two-hybrid (Y2H) assays were performed as described previously.⁵⁶ The full-length CDS of *OsEBF1* or *OsEBF2* was fused to pGBT7 to generate bait vectors (BK-OsEBF1 and OsEBF2) that contain the Gal4 DNA-binding domain. Full-length CDS of OsEIL5 were inserted into pGADT7 to produce prey vector (AD-OsEIL5) with the Gal4 activation domain. The bait and prey vectors were co-transformed into yeast strain AH109 and physical interactions were indicated by the ability of cells to grow on a dropout medium lacking Trp, Leu, His, and Ade for 5 d after plating. The primers used for the yeast constructs are listed in [Table S3](#).

Electrophoretic mobility shift assay

Plasmid construction and purification of GST-tagged OsEIL5 protein were performed as previously described.¹¹ Single stranded complementary oligonucleotide fragments containing putative OsEIL5-binding element (EBM1) from the OsPP91 promoter, or deliberately mutated binding sites, were synthesized and biotinylated (Sangon). Biotin-labeled and unlabeled oligonucleotide pairs were annealed to obtain double-stranded biotin-labeled and unlabeled probes by mixing equal amounts of each single-stranded complementary oligonucleotide fragment, incubating the fragments at 95°C for 5 min, and cooling them to room temperature slowly overnight. Probe sequences are given in Table S3. EMSA was performed using a LightShift Chemiluminescent EMSA Kit (Thermo Fisher) according to manufacturer's instructions. Reaction solutions were incubated for 20 min at room temperature. The protein-probe mixture was separated into a 5% native polyacrylamide gel and transferred to a nylon membrane. Following crosslinking under UV light, DNA on the membrane was detected using a Chemiluminescent Nucleic Acid Detection Module, according to the manufacturer's instructions.

Transactivation assay in tobacco leaves

Transactivation assay in tobacco leaves was performed as described previously.¹² The 1549 bp sequences upstream from the ATG codons of OsPP91 were cloned into binary vector pGWB435 to generate promoter:LUC reporter construct (pOsPP91:LUC). The cDNA fragment of OsEBF1 (1995 bp) was cloned into the pCAMBIA1300 vector to generate OsEBF1-3×Flag tagged construct. Different plasmid combinations of pOsPP91:LUC, 35S:EGFP, 35S:OsEIL5-EGFP, and 35S:OsEBF1-3×Flag were transformed into *Agrobacterium* strain GV3101, respectively. The strains were grown in LB medium and harvested by centrifugation. The cells were finally re-suspended in infiltration buffer with or without MG132 (10 mM MES, 0.2 mM acetosyringone, 10 mM MgCl₂, pH 5.6) to an ultimate concentration of OD₆₀₀ = 1.0. Equal amounts of bacterial suspensions were infiltrated into the leaves of 5-week-old *N. benthamiana* plants using a needleless syringe. After infection for 2 d, 1 mM precooled luciferin was sprayed on to the leaves, and then the samples were incubated in the dark for 5–10 min. The images were captured using a cooled charge-coupled device imaging apparatus. The luminescence were measured and quantified using ImageJ. The primers used are listed in Table S3.

ACC or ethephon treatment

To test ethylene reaction, the seeds of ZH11 and OsEIL5 transgenic lines were surface-sterilized with 3% sodium hypochlorite for 25 min, soaked at 35°C for 3 d. Germinating seeds were sowed into black 96-well plates without bottoms, and then each plate was placed on a black box filled with Kimura B nutrient solution containing 50 μM ACC or 150 μM ethephon. After 7 d of growth in the dark, the phenotypes were recorded, and the shoot length of these seedlings was measured.

ABA sensitivity analysis

To test ABA sensitivity, the seeds of ZH11, OsEIL5 transgenic lines, and ospp91 mutants were germinated on 1/2 MS medium for 3 d. After germination, the seedlings with similar shoot and root length were transplanted to transparent plastic plates with 1/2 MS medium containing 3 μM ABA or water as a control. After 8 d of growth, the phenotypes were recorded, and the shoot length of these seedlings was measured.

RNA-seq analysis

Approximately 14 d after germination, rice seedlings were transferred to 45°C, or kept at 28°C. After 6 h, seedlings were collected for each of the three replicates and immediately frozen in liquid nitrogen. Total RNA was extracted with TRIZOL. Sequencing libraries were generated using the NEBNext Ultra RNA Library Prep Kit for Illumina, followed by the RNA libraries sequenced on the Illumina sequencing platform by Genedenovo Biotechnology Co. Ltd (Guangzhou, China).

RNA-seq reads were aligned to the rice reference genome (https://ensembl.gramene.org/Oryza_sativa/Info/Index) using TopHat after filtering out low-quality (lowest base score <20) reads using SeqPrep and Sickle.⁵⁸ Gene expression level was calculated and normalized to FPKM (fragments per kilobase of transcript per million mapped reads) with RSEM.⁵⁹ Differential gene expression was determined using the R package edgeR.^{60,61} The cut-off for significant differential expression was set as log₂ (fold change) ≥ 1 and false discovery rate <0.05. The raw sequence data reported in this paper have been deposited in the Genome Sequence Archive (GSA: CRA018070) that are publicly accessible at <https://bigd.big.ac.cn>.

Luciferase complementation imaging assay

LCI assay was performed as previously described.⁵⁶ The pCAMBIA1300-nLUC and pCAMBIA1300-cLUC vectors were used for this analysis. The OsEIL5/OsEBF1/OsEBF2-nLUC and cLuc-OsEIL5/OsEBF1/OsEBF2 constructs were obtained by enzyme digestion and ligation or by seamless cloning. Different pairs of constructs were co-transformed into wild-type tobacco (*N. benthamiana*, 4 weeks old) leaves by *Agrobacterium* infiltration. After infection for 2 d, 1 mM precooled luciferin was sprayed on to the leaves, and then the samples were incubated in the dark for 5–10 min. The images were captured using a cooled charge-coupled device imaging apparatus. The primers used are listed in Table S3.

Bimolecular fluorescence complementation assay

The BiFC assay was performed as previously described.⁵⁶ To produce a fusion with either the N- or the C-terminal fragment of YFP, OsEIL5, OsEBF1, and OsEBF2 were subcloned into the pCAMBIA1300-nYFP or pCAMBIA1300-cYFP vectors, respectively.

Corresponding BiFC plasmids and negative controls were co-expressed in leaves of tobacco (*N. benthamiana*, 4 weeks old) expressing 35S:RFP-histone 2B (nuclear marker)³⁵ by *Agrobacterium* infiltration. After infection for 2 d, the YFP fluorescence was detected with a 514 nm laser (Leica TCS SP5). The primers used are listed in [Table S3](#).

Detection of OsEIL5 protein level

The EBF1R13, ZH11, and EBF1OE1 seedlings at 2.5–3.5 leaves stage were used to detect the protein levels of OsEIL5. Total protein was extracted with extraction buffer (50 mM Tris-HCl (pH 7.5), 100 mM NaCl, 1 mM EDTA, 10 mM NaF, 5 mM Na₃VO₄, 0.25% Triton X-100, 0.25% NP-40, 1 mM PMSF, 1× protease inhibitor cocktail) and adjusted to equal concentrations. OsEIL5 abundance was detected by western blotting using the anti-OsEIL5 antibody.

Analysis on the ubiquitination and degradation of OsEIL5

For OsEIL5 ubiquitination assay *in vivo*, rice protoplasts expressing OsEIL5-EGFP only or co-expressing OsEIL5-EGFP and OsEBF1-3×Flag were collected and grounded into fine powder in liquid nitrogen. Proteins were extracted in RIPA buffer with 100 μM MG132 and Protease Inhibitor Cocktail. The lysate was centrifuged at 12,000 r/min for 10 min at 4°C and supernatant were incubated with GFP-Trap beads for 6 h at 4°C. The beads were washed three times with PBS. The IP-product was resuspended in 1× SDS buffer and detected by western blot using anti-Ubi and anti-GFP antibodies.

The *in vivo* OsEIL5 degradation assay. Briefly, the *OsEIL5*-OE (OE9-3) seedlings at 2.5- to 3.5-leaf stage were transferred to the nutrient solution containing 300 mM CHX/DMSO or 300 mM CHX/50 μM MG132. Samples were harvested at the indicated time points for protein extraction. OsEIL5 abundance was detected by western blotting using the anti-OsEIL5 antibody.

The *in vitro* OsEIL5 degradation assay. Briefly, total proteins from ZH11 and EBF1R13 plants were extracted using degradation buffer (50 mM Tris-HCl pH 7.5, 150 mM NaCl, 0.5% NP40, 10 mM MgCl₂, 10 mM ATP) with or without 100 μM MG132, respectively. Then an equal amount of extract was incubated with purified GST-OsEIL5 protein at 28°C. At each time point (0, 15, 30 min), a 60 μL mixture aliquot was taken to conduct western blot analysis using an anti-GST antibody.

OsEIL5 protein degradation assay in the transient expression system was performed as described previously with some modifications.⁶² Different combinations of plasmids (OsEIL5-EGFP or OsEIL5-EGP/OsEBF1-3×Flag) were introduced into mesophilic protoplasts from wild-type ZH11 according to the Sheen laboratory protocol.⁶³ Transfected cells were cultured for 10 to 16 h with or without 50 μM MG132 treatment. And then, total protein was extracted with extraction buffer (50 mM Tris-HCl (pH 7.5), 100 mM NaCl, 1 mM EDTA, 10 mM NaF, 5 mM Na₃VO₄, 0.25% Triton X-100, 0.25% NP-40, 1 mM PMSF, 1× protease inhibitor cocktail) and adjusted to equal concentrations. OsEIL5 degradation was detected by western blotting using the anti-GFP antibody and OsEBF1 was detected using the anti-Flag antibody.

QUANTIFICATION AND STATISTICAL ANALYSIS

Statistical analyses were performed with Graphpad Prism 9.0 software. Data for quantification analyses are presented as mean ± standard error (SE) of mean, and 'n' represents number of samples from at least 3 replicates. Different letters indicate significant differences at $p < 0.05$, as determined by one-way ANOVA with Tukey's multiple comparisons test. The asterisks indicate significant differences from the controls by two-tailed Student's *t*-test (* $p < 0.05$, ** $p < 0.01$, *** $p < 0.001$, **** $p < 0.0001$). The details are included in the figure legends. Details about the statistical analyses are described in the figure legends.